University of Alberta

Study of Bio-densification Process in Oil Sands Tailings:
Modeling and Experimental Validation

by

Saba Roozbahani

A thesis submitted to the Faculty of Graduate Studies and Research
in partial fulfillment of the requirements for the degree of

Master of Science

in

Chemical Engineering

Department of Chemical and Material Engineering

Fall 2012
Edmonton, Alberta

Abstract

Slow densification of mature fine tailings (MFT) is one of the major challenges in reduction of tailings inventory, pore-water recovery and reclamation of tailings for oil sands industry. Bio-densification is a new treatment method in which densification of tailings is accelerated through microbiological activity.

Two-meter columns were installed to study effect of microbial activity on consolidation of MFT. Gas production and changes in concentration of ions due to microbial activity are recognized as two important parameters in settling rate of bio-activated tailings. Therefore, effects of these parameters on consolidation characteristics of tailings are studied. Effect of bicarbonate ions on settling was investigated based on a series of experiments on bitumen-free MFT which was synthesized through separation process. Two models have been developed based on finite strain theory to describe consolidation of saturated and gassy slurries. These equations are solved by COMSOL Multiphysics to predict the experimental observations.

Acknowledgments

This dissertation would not have been possible without the guidance and the help of several individuals who in one way or another contributed and extended their valuable assistance in the completion of this study.

First, I would like to thank my supervisor Dr. Rajender Gupta for giving me the opportunity to work on this project. I appreciate his patience, comments and suggestions. I have learned so much through this project. I would also thank Dr. Tariq Siddique for his comments and providing the opportunity to work in his lab.

I would like to express my gratitude to Ahad Sarraf Shirazi, my best friend, for all support, guidance, valuable comments, and encouragement.

I sincerely thank Shayan Karimipour and Arun K. Samanta for their assistant in this study. I also thank all members in our research group, Dr. Julia Foght, Alsu and Petr Kuznetsova, Rozlyn Young, Kathy Semple, for all supports.

Finally, I would like to thank Alberta Water Research Institute (AWRI) for the funding of this project.

Contents

List of Tables

List of Figures

Chapter 1

Introduction

Oil sands deposits in Northern Alberta were first discovered when the first explorer ventured into the Fort McMurray area in the 1760s. However, the commercial potential of these oil sands deposits has not been developed until 1920s. Two major extraction and refining plants were built between 1920 and 1959 to extract tar pitch oozing from the sand banks along the Athabasca River.

The Research Council of Alberta has played a key role in economical growth and development of oil sands; specially with pioneering work of Dr. Karl Clark in development of the process of bitumen extraction from oil sands. Dr. Clark and his research group constructed a bench-scale separation unit where they developed a hot water flotation process to separate the bitumen from the sand in the early 1924. Later on, different modifications have been done on the process through the 1920s to make it commercially viable (FTFC, 1995).

1.1 Oil sands

Crude bitumen, the valuable part of the oil sands, is a type of heavy oil with high viscosity at room temperature which makes it difficult to flow under gravity. The crude bitumen, the rock matrix, and any associated minerals are called oil sands (Masliyah, 2008). Currently, enormous amount of Canada's oil supply comes from oil sands deposits located in Province of Alberta. Athabasca deposit is the largest of the three oil sands area in Alberta (Athabasca, Cold Lake, Peace River Figure 1.1) with in-place reserves of about 27.6 billion cubic meters (175 billion barrels) of bitumen (ERCB, 2011).

Figure 1.1: Three major oil sands deposits (ERCB, 2011)

The existence of bitumen near the surface in the Fort McMurray area allows the deposit to be recovered by open pit mining. Essentially, the McMurray formation was deposited on the pre-Cretaceous on the Waterway Formation,

and it is subdivided into three zone that reflects environment of sediment deposition that grades from continental-fluvial (Lower), to tidal/estuary (Middle) and to tidal/marine (Upper). Basically, all bitumen reserves in the Athabasca deposit are contained within the lower zone of McMurray formation.

Typically, bitumen-bearing sediment consists of a mixture of coarse sand grains, fine mineral solids, clays, water and bitumen as shown in Figure 1.2. The amount of bitumen in the oil sands varies from 0 to 16 $wt\%$. Ores with bitumen content of 6 to 8% are considered as low-grade (poor) oil sands while with content above 10% are high-grade (rich) ores. Bitumen content of ores depends on particle size distribution of sands. The average amount of bitumen in the oil sands is 10 $wt\%$, and its recovery from the ores depends on the properties of the ores such as coarse and fine solid content, salt concentration and type of formation. Finer minerals including silt and clay present in low-grade ores disperse through Clark Hot Water Extraction process and mostly accumulate as fine tails deposits in the tailings (FTFC, 1995; Masliyah, 2008).

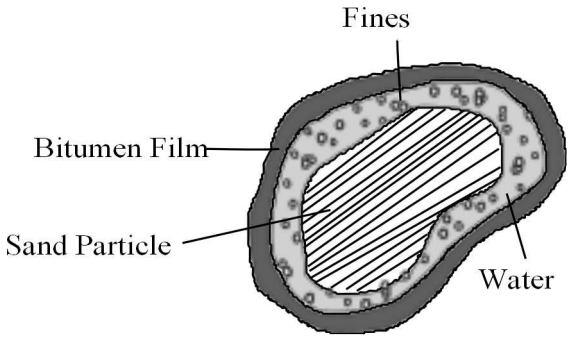

Figure 1.2: Schematic model for oil sands ore (modified from Masliyah (2008))

1.1.1 Mining operation

There are two commercial processes for bitumen production from the oil sands deposits under the ground; Open pit mining and in-situ production. In-situ production is applicable for oil sands deposits buried more than 100 meters and open pit mining for shallower deposits (less than 75 meters) (FTFC, 1995).

Early in the surface mining operation, the extraction of ore was done by draglines, bucket-wheels excavator, and conveyor belts. However, this operation changed from dragling/bucket-wheel/conveyor mining operation to shovel/truck/hydrotransport which is more energy efficient process in the early 1990s (FTFC, 1995; Masliyah, 2008).

1.1.2 Extraction process

The usual bitumen extraction process, referred to Clark hot water extraction (CHWE), is based on the pioneer work of Dr. Karl Clark. The combination of hot water, steam and caustic is used to separate the bitumen from the oil sands. After the mining process, dry mined ores are transported to the extraction plant where bitumen is separated. First, the ores are digested and conditioned in large tumblers with the addition of hot water, caustic soda ($NaOH$), and steam. The bitumen is separated from the sands (liberation) in this stage. At the tumbler discharge, rocks and clay-rich wastes are removed by vibrating screens. Although bitumen recovery of water is based on density difference, density of bitumen is very close to that of water. To resolve this problem, air is injected into the slurry in next step to ease the bitumen recovery. Aeration causes froth formation on top of the slurry, and bitumen would be collected as froth in large vessels, known as primary separation vessels. Bitumen froths,

separated in separation vessels, are first de-aerated, and its viscosity will be reduced by diluents. Bitumen froth contains significant quantity of water and fine solids, which must be removed prior to the upgrading process where bitumen is converted into a light synthetic crude oil (Masliyah, 2008; FTFC, 1995). The extraction process is illustrated in Figure 1.3.

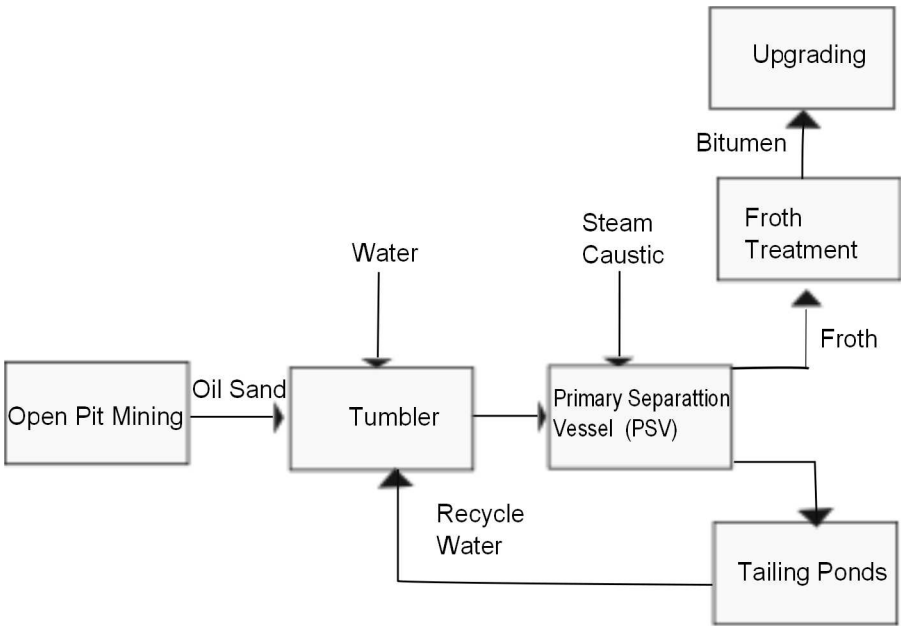

Figure 1.3: Bitumen Extraction Process (modified from FTFC (1995))

1.2 Statement of problem

Oil sands tailings are by-products of bitumen extraction process in Northern Alberta. Tailings, which consist of sand, silt, clay, and small amount of bitumen, are pumped to settling basins, tailing ponds, to densify. Most parts of sand (coarse particle) in the tailings settle down and leave fine particles ($< 44\mu m$) and bitumen (fine tailings) suspended in water. After few months of sedimentation, fine tailings concentration reaches to $20\,wt\%$ solid content. In next stage, fine tailings very slowly consolidate within two or three years,

and form mature fine tailings (MFT) with $30\,wt\%$ solid content. Over time, three areas form in the pond, which are clear water, fine tailings and mature fine tailings from top to bottom. Released water on the top is recycled to the extraction process to reduce usage of fresh water. Densification of MFT is estimated to require decades under in-situ condition. Due to the increasing volume of fine tailings, related environmental issues and increasing public concern, government of Alberta published a directive to regulate oil sands mining tailings operations (ERCB, 2009). A major problem associated with tailing deposits is the slow rate of sedimentation and consolidation. The required time for consolidation of fine tailings is predicted as 125-150 years (Eckert et al., 1996). To accelerate the process of densification, several chemical and physical approaches are investigated by industry, such as centrifugation and adding flocculants. However, some methods have side effects, for instance addition of gypsum results in emission of toxic H_2S, that requires seeking new alternatives.

Bio-densification is a new method to accelerate rate of densification, which is under investigation. Microbially-mediated densification is called "bio-densification". Microorganisms are active in the tailings and produce methane and carbon dioxide. This microbial activity increases the rate of densification of MFT (Fedorak et al., 2002). This phenomenon is under study as a new method for management of oil sands tailings.

1.3 Objectives

As discussed, laboratory and field observations proved faster densification due to natural anaerobic microbial activity in MFT. To investigate effect of microbial activity in settling behaviour of tailings, two-meter standpipes are installed, one with MFT and the other with bio-activated MFT. The objectives of this study are to:

1. Monitor different parameters including the settling rate and pore-water pressure in both standpipes.
2. Develop a model to predict the consolidation rate of mature fine tailings (MFT) and compare model predictions with experimental observations.
3. Investigate the effect of gas bubbles on the settling rate of bio-activated MFT.
4. Develop a model to predict the consolidation rate in gassy MFT and compare model predictions with experimental observations.
5. Predict the coefficient of compressibility and permeability for MFT and bio-activated MFT.
6. Study effect of bicarbonate ion concentration in the settling behaviour of MFT.

1.4 Organization of the Thesis

Chapter 2 is an overview of related topics such as origin of oil sands tailing, extraction process, and influential factors on slow rate of settlement, different methods for the treatment of tailings, and bio-activated tailings.

Chapter 3 reviews different approaches for the modeling of consolidation process in both saturated and gassy soil.

Chapter 4 describes different experiments such as consolidation and permeability tests, bitumen and organic removal from MFT, $2\,m$ and $2\,L$ slurry columns.

Simulation results and a comparison of model predictions with experimental results are discussed in Chapter 5.

Chapter 2

Literature Review

2.1 Oil sands tailings

The tailings from the separation vessels, floatation cells or cyclones are combined together and result in a warm aqueous suspension of sand, silt, clay, residual bitumen, and naphtha at a pH between 8 and 9. Tailings, mainly solids with particle size range of 0.1 to 300 microns and water, are pumped into large tailings ponds. In these ponds, coarse solids settle down to form dykes and beaches, and fresh water on the top is recovered and transferred to extraction process. Most of the fines and residual bitumen are carried into the pond as a thin slurry stream (about $3-8$ weight percent solid). The solid settlement is relatively fast, and after stream slows down, sedimentation of the particles begins. Stokian and hindered settlement of solid in the pond leave "free water zone" at the surface of the pond, which is recovered and recycled as extraction process water.

After the initial rapid settlement of larger particles, when fine mineral concentration reaches to a value close to 15 % by weight, the suspension develops

non-Newtonian properties. After 2-3 years of slow settlement, the tailings are called "Mature Fine Tailings (MFT)" with solid concentration of about 30 % by weight. It has very high viscosity with high yield stress, and consists of fine-grained material (silts and clays), water, and the residual bitumen. De-watering of MFT occurs very slowly, and it takes decades for it to reach consistency of soft soil. Since discharge of this material into the environment is not permitted, tailings will be stored in the ponds for further treatments. Currently, millions of cubic meters of tailings are stored in the tailings ponds, presenting a major environmental concern.

Over time, three zones develop in the tailings ponds as shown in Figure 2.1. Top zone, which is about three meters of clear water, is continuously pumped back into the extraction plant. Under the top layer is one meter transition zone that consists of water and settling clay particles. At the bottom is a layer of clays, fine sand, bitumen, and water, known as "fine tailings zone". In this layer, which can be as thick as $40\,m$ in some areas, density increases with depth. It is generally thought that the extremely slow consolidation of the fine tails is related to the dispersed nature of the fine and ultra fine particles as well as the ionic chemistry of the process water. Storage and disposal of large volumes of fine tails remains one of the major challenges associated with the Clark hot water extraction (FTFC, 1995; Masliyah, 2008).

It is better to do some calculations to get a better idea of how much tailings will be produced through the process. Practically about 2.0 tonnes of mined ore, and $2\,m^3$ of water (20 % fresh water and 80 % recycled water from the process) is needed to produce one barrel of bitumen. As a result, production of one barrel of bitumen results in 1.8 tonnes of solid tailings and $2\,m^3$of water-waste. It is anticipated that a tremendous amount of water is needed

to be recycled; otherwise it will cause problem for storage of tailings and providing fresh water for the process. Beside the slow settlement of the particles in the tailings, water in the tailings contains a large number of organic compounds, such as naphthenic acids and sulphonates and electrolytes, such as Cl^{-}, SO_4^{2-}, HCO_3^{-}, Ca^{2+}, $Mg^{2+} and\ Na^{+}$, which are produced during the extraction process. The presence of these organic compounds and electrolytes makes the tailing a highly toxic environment. Today, tailings management is a big challenge to environmentalists, scientists, and engineers in Alberta.

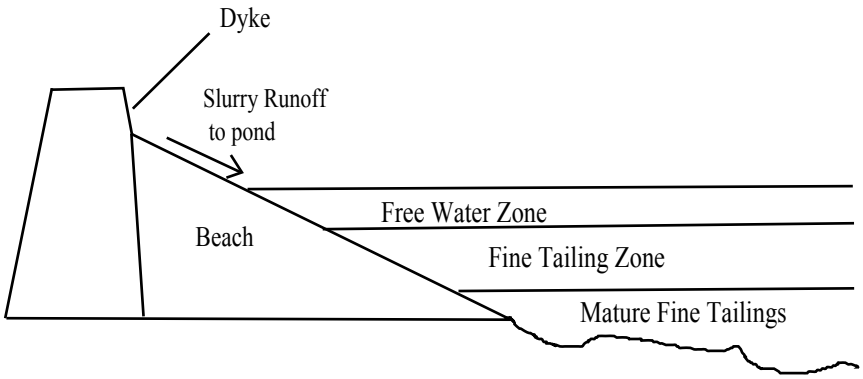

Figure 2.1: Schematic cross section of oil sands tailings suspensions (modified from Masliyah (2008))

2.1.1 Tailings composition

Oil sands tailings consists of six main components; water, sand (particles with size of more than 44 μm), silt (particles with the size of 2 to 44 μm), clay (particles smaller than 2 μm), bitumen, and naphtha (Kasperski, 1992). In addition, there is a small amount of heavy minerals and dissolved organics in oil sands tailings. Percentage of these components varies according to depth of tailings as shown in Tables 2.1 and 2.2.

	Overall composition (wt%)		
Depth (m)	Water	Mineral	Bitumen
11-13	82.0	17.1	0.9
14-17	75.7	22.9	1.4
18-22	69.2	28.4	2.4
23-27	60.5	36.3	3.2
>28	52.3	44.7	3.0

Table 2.1: Syncrude tailings pond composition, reported in 1986 (Kasperski, 1992)

	Particle Size Distribution		
Depth (ft)	%Sand($+44\mu$)	%Silt($2-44\mu$)	%Clay(-2μ)
20	1.9	50.1	48.0
45	13.5	51.6	34.9
60	44.6	31.3	24.1
70	47.5	34.5	18.0

Table 2.2: Particle size distribution of solids in oil sands tailings (Yong and Sethi, 1978)

The majority of clays in the tailings are kaolinite and illite as oil sands come from the McMurray Formation (Table 2.3). There are also traces of smectite, chlorite, vermiculite and mixed layer clays (Kasperski, 1992).

	Percent Minerals in Bitumen-Free Sludge Solids				
Depth (ft)	Kaolinite	Illite	Montmorilonite	Chlorite	Quartz
20	54.4	8.4	1.4	0.7	24.8
45	42.8	8.4	1.1	0.6	38.5
60	27.2	5.8	0.9	0.7	59.1
70	25.1	4.2	0.5	1.1	63.8

Table 2.3: Basic mineralogical analysis at various depths in the tailings pond (Yong and Sethi, 1978)

2.2 Influential factors in slow rate of settlement

After many years of research on tailings properties, it was concluded that the slow rate of settlement is inherent to the bitumen extraction process itself. This section focuses on effects of different parameters such as ore properties, temperature of extraction process, and concentration of sodium hydroxide used for extraction on the rate of consolidation.

2.2.1 Effect of ore properties

There is a considerable amount of fine particles in the tailings (Tables 2.2 and 2.3); therefore, it is essential to study their effects in slow settlement of tailings. It has been found that the fine particles are not individually suspended in the water phase, but they aggregate and form flocs (FTFC, 1995). These flocs start to settle; however, the rate of settlement decreases due to their interaction with each other. Also, the structure of fine tailings originated from the CHWE process is weak and does not have enough strength to tolerate any burden. This causes gel-structure and thixotropic property of tailings. Gel formation in the tailings happens fast and does not let coarser particles to be released; therefore, coarse particles will be entrapped in the gel structure which slows down the settlement of particles.

In addition to their physical properties, chemical composition of oil sands fine fraction affects the tailing. Oil sand fines contains compounds such as magnesium sulfate, calcium sulfate, and magnesium carbonate. Magnesium and calcium compounds require $NaOH$ to produce natural surfactants, which are essential in efficient recovery of bitumen from oil sands ore. Therefore, the more the fine contents is, the more $NaOH$ is required to produce enough

surfactant for bitumen separation (FTFC, 1995). Effect of sodium hydroxide on settling rate of tailings has been studied by Smith et al. (1994). They concluded that the amount of sodium hydroxide does not change the final volume of recovered water; however it changes the rate of settlement for the particles. They compared settling characteristics of tailings processed from the same ores. Tailings without $NaOH$ required about 10 days to reach to 50 % of settling point, however required time increased to 50 days for the one with 0.02 $wt\,\%$ $NaOH$.

2.2.2 Effect of temperature

Oil sands are processed at $80°C$ in standard Clark Hot Water Extraction process, which is the optimum temperature to recover maximum amount of bitumen from oil sand ores. Effect of operating temperature has been studied by Schramm and Smith (1989), and their results showed that operation temperature does not change settling behaviour of tailings.

2.2.3 Effect of surfactants

2.2.3.1 Interfacial tension

The work that is required to increase the surface area between two immiscible liquids by $\triangle A$ is defined as interfacial tension:

$$w = \gamma_{ab} \triangle A \tag{2.1}$$

where a and b indicate two liquid phases,

γ_{ab} is interfacial tension with dimension of $(\frac{N}{m})$.

In the case of bitumen extraction with hot water, imagine increasing surface area of water and bitumen by breaking a bitumen drop into two equal-size drops in water. The required work to achieve this surface increment between two phases increases when interfacial tension of these phases is high.

2.2.3.2 Surfactants

The term surfactant refers to a general class of substances called amphiphiles. Surfactants are components with two different regions; one region is water-soluble, i.e., hydrophilic, and the other is oil-soluble, i.e., hydrophobic. The hydrophobic region is usually consists of non-polar hydrocarbons, aliphatic or aromatic. The hydrophilic region consists of polar groups that interact strongly with water. The most important property of surfactants is their tendency to adsorb at surfaces; the hydrophilic region stays in water while the hydrophobic region stays in oily-phase. This phenomenon lowers the interfacial tension of water and oily-phase (Masliyah, 2008).

Natural surfactants such as naphthenates and sulfonates are produced during Clark Extraction process by $NaOH$. It has been hypothesized that natural surfactants play important role in toxicity and slow settlement of tailings (Smith et al., 1994). Dai and Smith investigated effects of natural surfactants in rate of settlement and toxicity of tailings by conducting series of experiments. He added calcium sulfate, which removes surfactant in the tailings, to different samples and studied their effects on toxicity and settling rates of tailings. The results showed significant increase in settling rate and reduction in toxicity of tailings. However, more studies are required for complete approval of this assumption. There are many factors that affect the settling rate of tailings, and they all should be considered. Some of these factors are discussed in this

work; however a detailed investigation of these parameters is beyond the goal of this project.

2.3 Different methods for management of tailings

Different approaches have been used for treatment of tailings such as physical, mechanical, chemical, geotechnical, and process modifications. Wet landscape reclamation was the initial industrial reaction (before 1989) for dealing with these accumulating tailings. In this process, mature fine tailings produced during extraction was transferred to the mined area and a layer of fresh water was added to the top to create an artificial lake. There are different disadvantages with using this method including oil floatation on the pond, expensive maintaining of the area, and toxicity of the tailings. Dry landscape is another treatment approach in which tailings are mixed by solid deposits and final landscapes become part of natural ecosystem. However, after 1989 researchers investigated other options that result in better densification of tailings. The most important alternative is consolidated tailings treatment that was commercialized by Suncor in 1994. Oil sands tailings have segregating characteristics as at initial stages of settlement, coarse solids separate from the rest and result in generation of fine tails zone. The settlement of this fine zone takes decades; therefore developing non-segregating tailings is desirable for faster reclamation. Addition of different salts is proposed as one of the options for producing non-segregating tailings by Liu et al. (1980). They studied settling behaviour of tailings by adding salts in different concentrations. They concluded that quick lime with concentration of $300 - 700 ppm$ improves settling

rate of tailings due to producing Ca^{+2}. However, gypsum ($CaSO_4.2H_2O$) is used commercially as a source of calcium ions because of the higher cost of lime. The final products of adding gypsum to tailings are referred as composite tails (CT). Other methods have been proposed as possible alternatives for treatment of tailings such as organic flocculent aids, high-intensity sound waves, changing pH, freeze-thaw, and bacterial treatment (Chalaturnyk et al., 2002). In the next part, some of these methods will be described in detail.

2.3.1 Treatment with divalent cations

The common divalent cation that is used for settlement of tailings is Ca^{+2}. This cation reduces repulsive forces among the particles that carry negative charges, and as a result particles coagulate. Therefore, Ca^{+2} is added to the tailings as a flocculating agent to make a non-segregating mixture that settles faster. One problem associated with this process is presence of calcium ions in the recycled water. Accumulation of Ca^{+2} in the process affects recovery of bitumen from ore sands as it changes interfacial tension of water and bitumen. Another problem is related to use of gypsum that increases SO_4^{-2} concentration which provides a favourable environment for bacteria to produce H_2S.

2.3.2 Treatment with changing pH

Hall and Tollefson (1982) investigated influence of changing pH on settling of tailings and found out that solids are settling faster below a critical pH. They added various components to tailings such as HCl, H_2SO_4, CO_2, or SO_2 to decrease pH. They concluded that the main reason for faster settlement is reduction of HCO_3^- due to increase in H^+ concentration. However, change in

pH was not used as a possible option due to high cost of process and difficulty of bitumen recovery in acidic environment (Kasperski, 1992).

2.3.3 Treatment by using bacteria

Mittal (1981) proposed the idea of using available bacteria in tailings for faster consolidation. The bacteria can be used for removal of bitumen in the tailings as it was studied by Hocking (1971). Hocking found faster settlement of tailings with addition of nutrients. This method is the main focus of this study and it will be discussed in detail.

Beside chemical and mechanical methods, other treatments are used to enhance rate of settling such as adding different composition of coarse solids, using swelling properties of clays in overburden; however each treatment has its own advantages and disadvantages, and new methods are under investigation.

2.4 Microbially-mediated tailings

Oil sands tailing is an anaerobic environment and similar to other anaerobic systems contain different groups of microorganisms. Two main organisms that are recognized in the tailings are sulfate-reducing and methanogens bacteria. Methanogens reduce CO_2 by using hydrogen as electron donor and produce methane. In presence of SO_4^{-2}, sulfate reducing bacteria (SRB) have more energy coming from the reduction of sulfate. Therefore, they have more advantages compare to methanogens for using electron donors such as hydrogen. After depletion of sulfate, methanogens have more advantage because of their faster growth rate and start growing their community (Raskin et al., 1996).

Mildred Lake Settling Basin (MLSB) is one of Syncrude Canada Ltd. settling basins which was established from beginning of Syncrude‘s operation in 1978. Gas production was first recognized in early 1990s in Southside of this lake; however it gradually spread across all over the lake. The gas analysis showed that about 60-80% of this gas flux across MSLB is methane (Holowenko et al., 2000). Methane is an air pollutant and one of the greenhouse gases, therefore its production in the lake increased awareness among researchers.

2.4.1 Methane production in oil sands tailings

Foght et al. (1985) conducted the first series of analysis on the microbial community in MSLB, Syncrude‘s tailings pond. The results showed existence of both anaerobic and aerobic microorganism such as sulfate-reducing and in specific condition, methanogens. After observation of methane production from the tailings in MSLB, researches conducted different experiments on gas production and bacterial activity in tailings. According to initial results, it was concluded that methane production disturbs the tailings and reduces settling rate of particles. However, more investigations showed the opposite results. For the matter of methane production (methanogenesis), substrates and suitable conditions should be provided for bacteria in mature fine tailings (MFT). Fedorak et al. (2003) claimed rapid densification of MFT with methane production compared to non-methanogenic MFT. They compared settling results from their columns filled by methanogenic tailings to the one from Syncrude Research, non-metanogenic, and concluded faster settlement in methanogenic tailings. These observations initiated new series of investigations on bio-activated tailings toward improvement of settling rate of MFT which will be discussed in following section.

2.4.2 Effect of gas production on tailings properties

It is essential to study the properties of gassy (unsaturated) MFT in order to understand influential factors which are causing faster consolidation of tailings. Syncrude Canada Ltd. started monitoring MFT properties such as temperature, gas production, pH, electrical conductivity (EC), chemical parameters and ion concentration at three different stations in MSLB. These measurements provided valuable insight into chemical and physical properties of tailings ponds (Guo, 2009).

2.4.2.1 Temperature

Syncrude Canada Ltd. measured the temperature in different depths of three stations at MSLB and the results were reported by Guo (2009). The data showed tailings temperatures between 10^oC to 16^oC with small variation before 1994. However, the temperature increased rapidly from 1994 to 1997 and reached 23.5^oC . This increase in temperature had a huge influence on the microbial activity in the pond as the optimal range of temperature for methanogenesis is reported from 33^oC to 35^oC (Cooper and Harrington, 1988). Guo (2009) reported two possible reasons for this increase in temperature; heat generation from microbial activity, and the discharge of oil sands tailings with higher temperature to the tailings ponds. However, he concluded that the external factor such as the temperature of discharged tailings could be the major reason for temperature rising as the microbial activity does not affect tailings temperature significantly.

2.4.2.2 Gas production

Gas content of tailings is measured by Syncrude Canada Ltd. since 1996, and the results showed rapid increase from 1996 to 1999 in the depth of 5 to 10 m below MFT-water interface. Guo (2009) reported the maximum gas production at about $5-6$ m below surface by observing the data from different stations with time. Also, he suggested that the most intense microbial activity is happening at this depth in which the densification of tailings is the most significant.

2.4.2.3 Hydrogen concentration

The pH value is an important factor in chemical and physical properties of tailings. Gustafsson et al. (2001) investigated effect of pH changes in rheology of the sediments. Decrease in pH reduces repulsive forces among clays and makes their coagulation easier, which results in faster settlement. The values of pH have been measured in two different depths for different stations by Syncrude. The data showed decrease in pH values from 8.6 to 7.8 from 1992 to 2003, which can be attributed to dissolution of CO_2, produced due to biological activity, in tailings water (Guo, 2009).

2.4.2.4 Electrical conductivity (EC)

Electrical conductivity measured in the tailings showed an increase in pore water salinity as a result of biological activities. The concentration of different ions, both cations and anions, were measured in different stations over time. Cation measurement in the tailings showed increase in Na^+, Ca^2, Mg^{2+}concentrations in the stations from 1993 to 2001. Guo (2009) proposed

different reasons for increase in ion concentration including change of minerals in oil sands ores, changes in extraction process, reuse of released water for extraction process, increase in temperature, and decrease in pH .

Among anions, bicarbonate HCO_3^- is the most abundant ion, and it affects the settling behaviour of MFT. The concentration of bicarbonate increased in the tailings pond from 1991 to 2003. Sulphate is another anion present in the tailings that is very important in microbial activity. Increase in the concentration of sulphate decreases methanogenesis and reduces methane production (Fedorak et al., 2000). The concentration of sulphate in the tailings reduced over time since 1985, which is another indicator of biological activity in the tailings.

Also, concentration of Naphtha decreased from 1996 to 2002 in the pond. This component is a chemical added in the extraction process to facilitate bitumen recovery, and it flows to the pond with tailings water (Guo, 2009). Sidique et al. (2007) proposed that the bacteria in tailings pond uses naphtha and supports the methanogenesis as a result.

In the next chapter, different modeling approaches are studied for prediction of settlement of MFT with and without gas.

Chapter 3

Modeling

3.1 Introduction to settlement of suspension

Oil sands tailing mainly consist of water and solid particles, therefore its settling process is similar to settlement of particles in suspension of soil, which is referred to a well distributed mixture of soil particles in water. The process of settlement consists of three stages; flocculation, sedimentation and consolidation. At initial stage, flocculation, particles tend to cohere and form flocs which are clusters of particles and confined water. In the next stage, sedimentation, flocs gradually settle down under their gravity. Sedimentation is the process in which dispersed particles fall through the fluid and form sediment. In tailings pond, both Stokian and hindered settling take place in the sedimentation zone in which solid content increases from 8 to 20 $wt\%$ (Yong et al., 1983). Finally, each layer of soil sediment goes under weight of the overlying sediment and consolidates (Imai, 1981). Consolidation is process of deformation of a system of particles under an imposed force. This force could be due to self weight of the bulk system or an external surcharge loading (Schiffman

et al., 1985). In the tailings, consolidation happens in solid content of 15 to $20\,wt\%$ when solids start to form a matrix in which stress can transfer from one particle to another. After this point, self weight consolidation is the only source of increase in solid content. Through this process, solid content of tailings reaches to $30\,wt\%$ in about two years. At this point, tailing is called mature fine tailings (MFT) and rate of consolidation decreases dramatically afterwards (Chalaturnyk et al., 2002).

Settling of particles in suspension is common to different industrial and natural processes such as soil sedimentation, management of tailings, and gravity thickening. Up to now, lots of studies have been done for better understanding of nature of the process. These studies started with chemical engineers who tried to understand fundamentals of sedimentation and continued by geotechnical engineers who focused more on consolidation process.

In next section, process of sedimentation and consolidation are discussed from chemical and geotechnical point of view.

3.2 Sedimentation

The concept of sedimentation was discussed by chemical engineers due to wide range of applications in chemical processes. The first step to describe the process of settlement is to consider forces which are acting on an individual spherical particle.

These forces were first studied by Stokes in 1851. He derived an equation for the resistance force acting on spherical particle which comes from its movement through viscous fluid (Richardson and Zaki, 1954).

$$F = 3\pi\mu V d \tag{3.1}$$

where F is viscous drag, d is diameter of sphere, μ is viscosity of fluid, and V is velocity of sphere relative to fluid.

There are three forces acting on a particle; gravity, buoyancy, and drag force (Figure 3.1). Force balance on particle equates terminal velocity of spherical particle in the viscous fluid.

I.e.

$$V = \frac{d^2\left(\rho_s - \rho_f\right)g}{18\mu} \tag{3.2}$$

where ρ_s =density of sphere,

ρ_f = density of fluid,

and g = acceleration due to gravity.

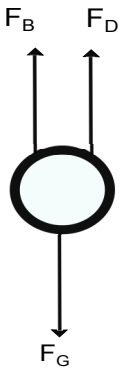

Figure 3.1: The forces acting on a single particle

Equation 3.2 is based on Stokes drag force, and only depends on the specific gravity, particle size and viscosity of fluid. Stokes equation is only appropriate for single particle in laminar flow system ($Re < 1$). However, there are particles interactions in a real suspension which results in slower settlement of suspension.

The initial studies on settling velocity of particles in suspension have been done by Einstein (1911) for very dilute suspension (Kynch, 1952). He derived a formula for settling velocity of particles in dilute suspension as

$$v = u_{\infty}(1 - \alpha.c) \tag{3.3}$$

where α is 2.5 for hard spheres,

u_{∞} is Stokes velocity,

and c is volume concentration.

Different modifications have been done on Stokes formulation to predict the settling velocity in suspension. For instance, Robinson in 1926 proposed a modification for Stokes law to predict settling rate of suspension for uniformly sized particles;

$$V_c = K\frac{d^2\left(\rho_s - \rho_c\right)g}{\mu} \tag{3.4}$$

where ρ_c is average density of suspension,

V_c is settling velocity of particles in suspension,

μ is viscosity of suspension,

and K is constant.

Equation 3.4 is proper for spheres with uniform size and density which are well-distributed in the fluid. It predicts particles velocity in suspension by

multiplying a constant factor to the Stokes particle velocity. The constant parameter is calculated according to characteristic of suspension, which is not convenient.

Steinour (1944) studied the sedimentation of uniform particles and described the equation for settlement of particles in term of solid concentration. He modified the Stokes equation as

$$V = \frac{2gr^2\left(\rho_s - \rho_c\right)g\epsilon^2\phi\left(\epsilon\right)}{9\mu} \tag{3.5}$$

where $\phi\left(\epsilon\right)$ = represents effects of size, shape, and flow space,

and ϵ= fluid volume fraction.

Steinour (1944) estimated $\phi\left(\epsilon\right)$ according to his studies on sedimentation of particles in oil

$$\phi\left(\epsilon\right) = 10^{-1.82(1-\epsilon)} \tag{3.6}$$

Therefore

$$V = \frac{2gr^2\left(\rho_s - \rho_c\right)g\epsilon^2}{9\mu}10^{-1.82(1-\epsilon)} \tag{3.7}$$

However, Steinour (1944) assumed that buoyancy force exerting on particles depends only on density of suspension, which cannot be correct as each particle only can displace the water equal to its volume after it settles. Richardson and Zaki (1954) proposed an equation for settlement of particles in the suspension in which they included particles characteristics;

$$V_c = V_0\epsilon^n \tag{3.8}$$

where $V_c = falling\, velocity\, of\, suspension$

They investigated effect of particle shape on their settling characteristics, and estimated value of n equals to 4.695. Kynch (1952) realized the transient nature of process and presented the hindered settling for settlement of particles. He assumed that the falling velocity of a particle depends on local concentration of particles at that point. He derived an equation based on the continuity of solids and ignored effective stresses and other forces formed at the bottom. The sedimentation equations are based on Kynch's theory. In the following sections, the equations for sedimentation and consolidation in suspension are discussed.

3.2.1 Sedimentation equations

Sedimentation of suspension depends on size distribution of particles, density, and surface properties of particles in the slurry. Imagine settlement of particles in the slurry with size of $1\,mm$. There is not any yield or strength against settling in this slurry due to the large size of particles. They form sediment layer and clear water on top. Now, consider batch settling of fine particles with diameter of 24 μm or less. There are attractive and repulsive forces among particles. The attractive force such as London-van der Waals causes floc formation in the slurry. These flocs form a gel-like network that can transmit stress and in other words can yield stresses in the slurry. If the applied stress on the network increases to more than strength of network, it will collapse and form sediment with new concentration that can support new applied stress. This new layer forms at the bottom of slurry and consolidates over time. Therefore, three layers of clear water, suspension, and sediment form during settling of suspension that are illustrated in Figure 3.2 (Eckert et al., 1996).

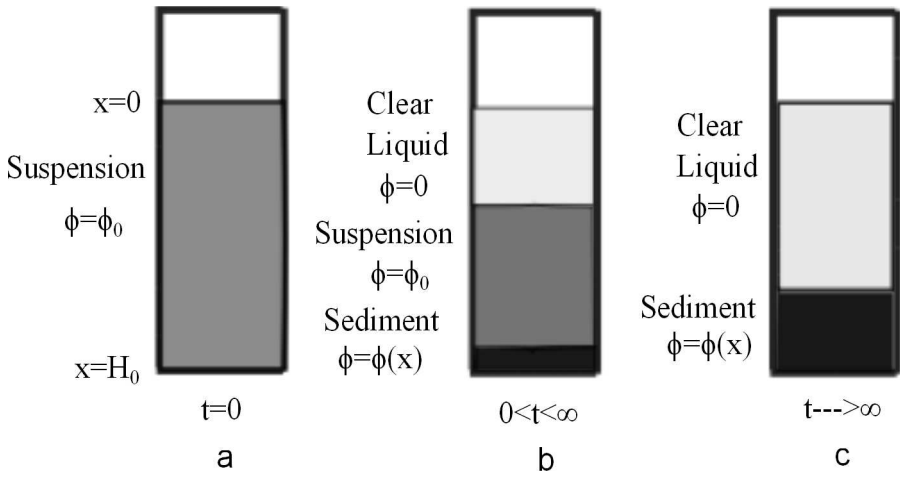

Figure 3.2: Suspension settling a) initial state; b) intermediate state; c) final state (modified from Eckert et al. (1996))

Buscall et al. (1982) developed mathematical equations for sedimentation and consolidation of suspension by considering chemical engineering or fluid dynamics point of view. They modified Kynch equation for hindered settling, and added the effect of strength of suspension. To compare the results of experiment with the theory, Buscall et al. (1982) introduced centrifuge techniques for measuring compressive yield stress and hindered settling velocity as a function of solid volume fraction. However, solid volume fraction for different locations is required to calculate the final results. Auzerais et al. (1988) questioned consistency of a range of systems and initial conditions of Kynch's theory, and developed two equations for movement of interface between sediment-suspension and suspension-clear water. Later on, Eckert et al. (1996) applied experimental procedure by Buscall et al. and theoretical equations by Auzerais et al. (1988) to calculate settling rate of fine tailings. They considered an horizontal element of sample in the network and equated the forces on the element (Figure 3.3).

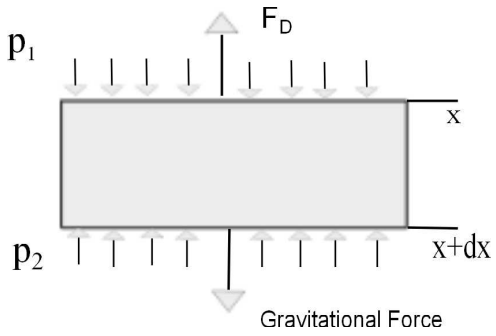

Figure 3.3: Forces acting on an element (modified from Eckert et al. (1996))

Force balance on the element equated as (Eckert et al., 1996)

$$Stress\,on\,the\,network - gravitational\,force + drag\,force = 0 \tag{3.9}$$

$$-\frac{\partial P}{\partial x} + (\rho_s - \rho_f)g\phi - \frac{\lambda_{st} a_p \mu \phi r(\phi)}{V_p}(v_s - v_f) = 0 \tag{3.10}$$

where P is stress on the element, $\rho_s\,and\,\rho_f$ are density of solid and fluid respectively, ϕ is volume fraction of solid, λ_{st} is Stoke's drag coefficient, a_p characteristic dimension of single particle, μ is viscosity of fluid, $r(\phi)$ is interaction function that is introduced by Buscall and White, V_p is volume of particle, v_s and v_f are velocity of fluid and solid respectively, and x is spatial coordinate of the system.

The first step is to calculate fluid velocity based on solid velocity and substitute it in the force balance. In order to find this relationship, continuity equations of solids and fluid are combined with mass conservation of liquid and solids in a closed system.

As a result force balance of network changes to

$$-\frac{\partial P}{\partial x} + (\rho_s - \rho_f)g\phi - \frac{\triangle \rho g \phi r(\phi)}{U_\infty (1-\phi)} u_s = 0 \tag{3.11}$$

where U_∞ is Stokes settling velocity of single particle, and is defined as $U_\infty = \frac{\triangle \rho g V_p}{\lambda_{st} a_p \mu}$.

The hindered settling velocity is applied for suspension

$$U(\phi) = \frac{U_\infty (1-\phi)}{r(\phi)} \tag{3.12}$$

By combining equation 3.11 and 3.12, the velocity of solid particles would be

$$v_s = U(\phi)(1 - \frac{1}{\triangle \rho g \phi} \frac{\partial P}{\partial x}) \tag{3.13}$$

Equation 3.13 is valid for both sediment and suspension zone. At initial stages of settling, solid velocity is equal to hindered settling velocity due to presence of uniform particles concentration in suspension. As explained earlier, when applied pressure exceeds yield stress of network, it collapses to a denser concentration to support new stress. Therefore, applied pressure can be replaced by compressive yield stress in equation 3.13. Eckert et al. (1996) solved the equations and calculated settling rate of sedimentation and consolidation in batch settling. They substituted Stokes velocity and yield stress of network for fine tails according to centrifugation procedure introduced by Buscall et al. (1982). They also compared their final equations with finite strain equation by Gibson et al. (1989), and pointed out the similarities.

As process of sedimentation is already completed in MFT, equations of sedimentation are not solved in this work. In following section, equations of con-

solidations are discussed in the form of effective stress, void ratio and hydraulic conductivity (Geotechnical Engineering point of view).

3.3 Theories of consolidation

At beginning of this part, concepts of flocculation, sedimentation, and consolidation are described. As Schiffman et al. (1985) defined:

"Flocculation refers to the particles in the system which tend to cohere.

Sedimentation is the process of particles settlement in the fluid suspension under the force of their gravity.

Consolidation is the process of deformation of mineral skeleton under the action of an external force. This external force could be the weight of upper layers (soil or fluid) or an imposed load."

Imai (1989) described the process of flocculation/sedimentation/consolidation as:

"In the first stage, no settling takes place, but flocculation yields flocs. In the second stage, the flocs gradually settle and form a layer of sediment, which undergoes consolidation and reduction of water content. The boundary between the upper settling zone and the sediment is the birth place of new sediment. While the sediment grows, the settling zone became thinner and finally vanishes. In the last stage, all of sediment thus formed undergoes self-weight consolidation and finally approaches an equilibrium state." These three stages are illustrated in Figure 3.4.

There have been a lot of efforts to demonstrate deformation of a porous medium (clay) filled by fluid (water) with mathematical equations. The process of con-

solidation happens when a compressive force acts on porous medium consists of solid particles and water. Initially, the external force compresses pore-water in the clay skeleton, and causes development of excess pore water pressure. Water flows out due to hydraulic gradient which is caused by excess pressure. This excess pressure will gradually dissipate and will change the volume of soil. The process of compression of porous material which caused pore-water removal and solid deformation is called consolidation, and the final governing equations are called theory of consolidations (Schiffman).

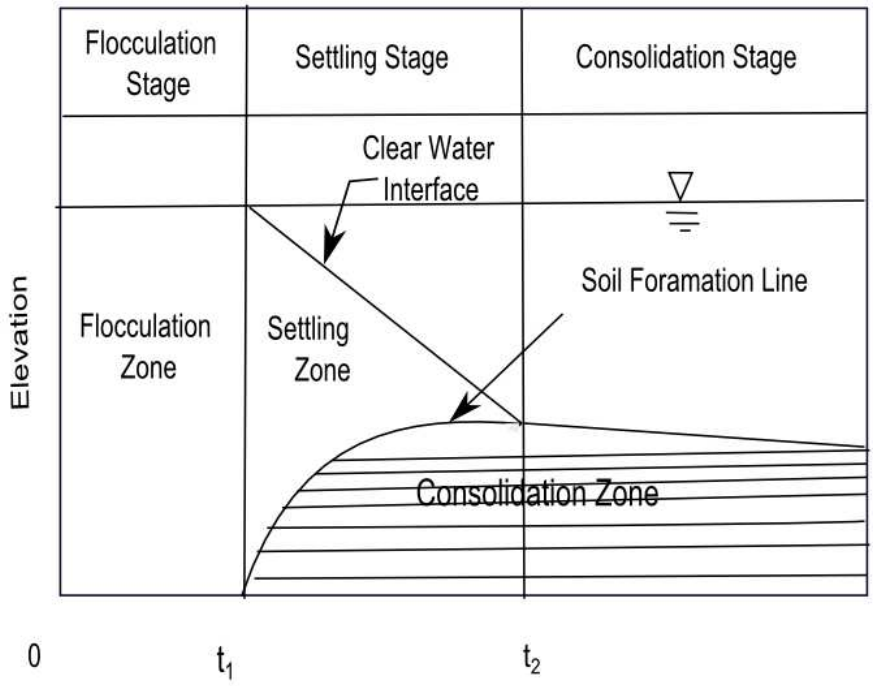

Figure 3.4: Flocculation, sedimentation, and consolidation process (modified from Imai (1981))

3.3.1 Review on theories of consolidation

Knowledge of the coordinate systems and fundamental parameters of consolidation are essential to understand the governing equations of consolidation.

3.3.1.1 Coordinate systems

Tailing is a solid-fluid media in which each phase is moving relative to the other. There are three coordinate systems that are common for such systems; Eulerian, Convective and Reduced coordinates.

In Eulerian coordinate system, deformations and movements are related to the fixed datum plane in space. This coordinate is proper when deformation of soil is negligible compared to the thickness of sample. However, during consolidation deformation of material is considerable; therefore Eulerian coordinate is not suitable. Gibson et al. (1967) applied Convective and Reduced coordinates to formulate consolidation.

The process of consolidation for an element of soil is illustrated in Figure 3.5. Before the consolidation begins, soil layer has a dimension of $A_0B_0C_0D_0$, with coordinate position of a and thickness of δa. The bottom boundary is fixed and its coordinate position is $a = 0$, and the upper boundary is at $a = a_0$. The dimension of sample will change to $ABCD$ by deformation of clay as a result of consolidation. After consolidation, at time t, clay layer is located at $\xi(a, t)$. This new position of clay layer is a function of time and is considered as Convective coordinate. It is more convenient to express our equations in Convective coordinate from physical points of view, but it would be hard to solve the equations while independent variable is changing by time.

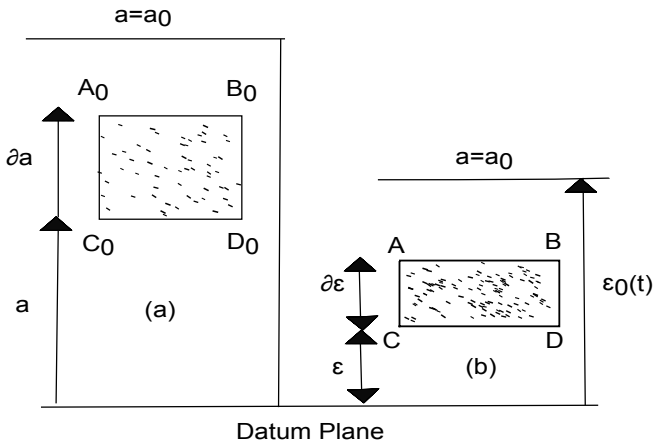

Figure 3.5: Eulerian and convective coordinates; a) sample layer at t=0; b) layer at time t (modified from Schiffman et al. (1985))

To overcome difficulties of Convective coordinate, reduced coordinate system (z) is defined, which is based on volume of solid lying between datum plane and any point under study (McNabb, 1960). In reduced coordinate, focus is on the solid particles rather than one point in the space. As volume of solid is constant all the time, use of this coordinate system is proper to avoid moving coordinates. Reduced coordinate (z) is independent of time and defined as

$$z(a) = \int_0^a [1 - n(a', 0)]\, da' \tag{3.14}$$

where n is the porosity of the system

$$e = \frac{n}{1-n} \tag{3.15}$$

In terms of void ratio ($e = \frac{volume\,of\,fluid}{volume\,of\,solid}$), reduced coordinate will be defined as

$$\frac{dz}{da} = \frac{1}{1+e_0} \tag{3.16}$$

where e_0 is the void ratio at initial condition ($t = 0$).

Transformation between these two coordinates, Reduced and Convective, is given by

$$\partial z \rho_s(z, 0) = \frac{\partial \varepsilon \rho_s(z, t)}{1 - n(z, t)} \tag{3.17}$$

where ρ_s is density of solid phase.

3.3.1.2 Consolidation parameters

Effective stress, permeability, and excess pore-water pressure are fundamental parameters that help to get a better understanding of theories of consolidation. Effective stress is responsible for deformation of porous system, and it was first defined by Terzaghi (1936). He described it as " the total stress in a saturated (porous material) consists of two parts with different mechanical effects. One part, which is equal to the pressure in the (pore) water produces neither a measurable compression... . This part is called pore-water pressure u_w ... . The second part σ' is called effective stress because it represents that part of total stress which produces measurable effects such as compaction or an increase in shearing resistance..." (Terzaghi, 1943).

Effective stress causes deformation and volume changes in saturated tailings which result in development of stress in the system. This parameter is related to total stress and pore water pressure by the equation

$$\sigma = \sigma' + u_w \tag{3.18}$$

where σ is total stress on the system, u_w is pore water pressure (which is partial pressure for water), and σ' is effective stress.

Excess pore water pressure is defined as excess pressure over hydrostatic pressure of water. It can be also defined as pore-water pressure in excess of a steady-state flow condition (Schiffman, 2000).

$$u = u_w - u_s \tag{3.19}$$

where u_s is hydrostatic pressure, u_w is pore-water pressure, and u is excess pore-water pressure.

To illustrate the meaning of excess pore-water pressure, imagine a piezometer inserted in a layer of clay as illustrated in Figure 3.6. At $t = 0$, consolidation in soil has not started yet, therefore water pressure at any point in soil is equal to hydrostatic pressure at that point. After soil consolidates, pore-water pressure increases in soil. This extra pressure due to consolidation is called excess pore pressure. By using the definition described by Gibson et al. (1989) total head at any point is

$$h = h_e + h_p \tag{3.20}$$

where h is total head, h_e elevation head, and h_p pore pressure head.

The pore-water pressure consists of static pressure and excess pore-water pressure. Therefore, the equation (3.20) changes to

$$h = h_e + \frac{1}{\gamma_w}(u_s + u) \tag{3.21}$$

where u_s is static pressure of water, and u excess pore-water pressure.

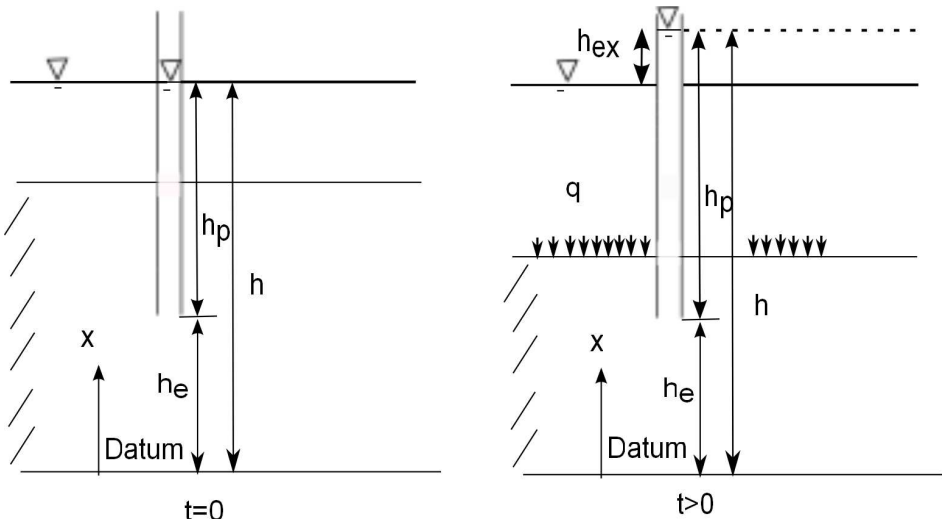

Figure 3.6: Definition of excess pore-water pressure (modified by Gibson et al. (1989))

Terzaghi (1924) defined hydraulic conductivity as " The reduced [hydraulic conductivity, k_z] is the speed with which the water would percolate through the sample if the difference between the two water levels were [H_z] instead of [H]. This speed of percolation is obviously smaller than the true [hydraulic conductivity]. Since, according to Darcy's law, there exists a simple proportionality between the hydraulic gradient and the speed of percolation."

There are two aspects of the consolidation theory, infinitesimal and finite strain, that are described in following part before discussion on different theories. In infinitesimal strain concept, it is assumed that deformation of clay during consolidation is small compared to its thickness. Therefore, consolidation parameters are calculated based on a fixed point in space as a function of time which means use of Eulerian coordinate system.

Finite strain theory of consolidation has no restriction on the magnitude of deformation during the process. As deformation of soil during consolidation is significant compared to its thickness, use of a fixed coordinate is not proper.

For this system, dependent variables are calculated in terms of Convective or Reduced coordinate system.

Terzaghi formulated one-dimensional consolidation based on finite strain theory for the first time in 1923, but he assumed that compressibility and reduced coefficient of permeability are constant (Terzaghi, 1924). His theory is not applicable for a soft soil that consolidates under its own weight as self-weight consolidation causes large strains which results in changes in compressibility and permeability of soft soil.

Terzaghi reformulated one-dimensional consolidation based on infinitesimal theory in 1942. He made following assumptions;

1. The soil is saturated and homogeneous.
2. The pore fluid is incompressible.
3. Compression of soil and average flow are one-dimensional.
4. The Darcy‘s law is applicable for permeability of soil.
5. Coefficient of permeability is constant over time during consolidation.
6. The void ratio is not a function of time and only changes with vertical effective stress.
7. The coefficient of compressibility is constant during consolidation.
8. Vertical deformations of soil are small during consolidation compared to its thickness.

Terzaghi developed one-dimensional theory of consolidation according excess pore-water pressure as

$$\frac{\partial u}{\partial t} = c_v \frac{\partial^2 u}{\partial x^2} \tag{3.22}$$

where u is excess pore water pressure,

x spatial coordinate,

and c_v coefficient of consolidation.

$$c_v = \frac{k(1+e_0)}{a_v \gamma_w} \tag{3.23}$$

where a_v is compressibility coefficient.

Different studies have been done to modify Terzaghi's equation, and avoid errors which arise from assuming constant compressibility and hydraulic conductivity. Gibson et al. (1967) eventually developed one dimensional non-linear finite strain theory. The finite strain theory is applied for simulation of consolidation of MFT in this study.

3.3.2 Finite strain theory

A homogeneous soil layer with initial thickness $h(0)$ is considered (Figure 3.7) to examine progress of consolidation. To derive the equation of consolidation, an element of soil skeleton has been selected with unit cross-sectional as illustrated in Figure 3.5. The element has the Convective coordinates of ξ and void ratio of e , which is the volume of fluid per volume of solids. For this element, $ABCD$ in Figure 3.5, the vertical equilibrium of soil grains is

$$\frac{\partial \sigma}{\partial \xi} + \left[\frac{e\rho_f + \rho_s}{1+e}\right] = 0 \tag{3.24}$$

where σ is vertical total stress,

ρ_f is density of fluid,

and ρ_s is density of solid.

(the coordinate system is against gravity)

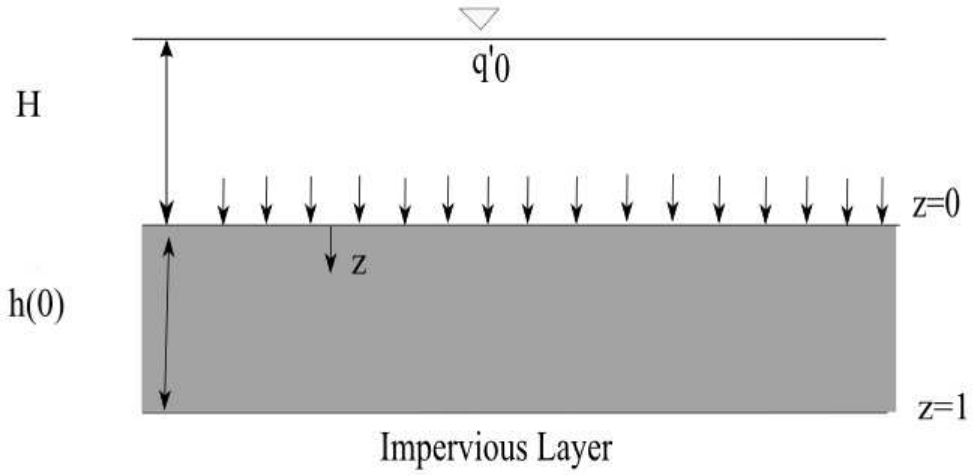

Figure 3.7: Thick and homogeneous clay layer (modified from Gibson et al. (1989))

The rate of outflow fluid must be equal to change in rate of fluid in that element to derive vertical equilibrium relation for pore fluid.

Therefore, final equation for fluid equilibrium is

$$\frac{\partial}{\partial z}\left[\left(v_f - v_s\right) e\rho_f\right] + \frac{\partial}{\partial t}\left[e\rho_f\right] = 0 \tag{3.25}$$

where v_f is velocity of fluid,

and v_s is velocity of solid.

3.3.2.1 Continuity equations

There is continuity equation for solid, liquid phase and mixture of both in MFT.

For solid phase

$$\frac{\partial}{\partial \xi}(\rho_s(1-n)v_s) - \frac{\partial}{\partial t}(\rho_s(1-n)) = 0 \tag{3.26}$$

For liquid phase

$$\frac{\partial}{\partial \xi}(\rho_f n v_f) - \frac{\partial}{\partial t}(\rho_f n) = 0 \tag{3.27}$$

where n is porosity of mixture ($n = \frac{volume\,of\,fluid}{volume\,of\,mixture}$).

By adding the equations of continuity for solid and liquid, the continuity of mixture results in

$$(1+e)\frac{\partial}{\partial \xi}\left[n\left(v_f - v_s\right)\right] + \frac{\partial e}{\partial t} + v_s\frac{\partial e}{\partial \xi} = 0 \tag{3.28}$$

$$\frac{De}{Dt} = \frac{\partial e}{\partial t} + v_s\frac{\partial e}{\partial \xi} \tag{3.29}$$

In our system, the fluid and solid are assumed incompressible that means ρ_s and ρ_f are constant.

3.3.2.2 Darcy-Gersevanov's law

To drive final equation of finite strain, we need an equation to relate velocity of water to its pressure. Darcy's law for movement of fluid through porous media is applicable for our laminar system. However, there should be some modifications on the original equation, to satisfy physics of the system. Drag force on the solid particles is not only a relation of solid velocity nor fluid velocity alone, but it is a relation of relative velocity $(v_w - v_s)$ in our system (Gibson et al., 1967). Therefore, modified equation by Gersevanov (1934) is used;

$$n(v_f - v_s) = \frac{k}{\rho_f}\frac{\partial u}{\partial \xi} \tag{3.30}$$

where k is the coefficient of permeability,

and u is excess pore pressure of fluid.

3.3.2.3 Final formulation

There are some assumptions associated with finite strain equation of consolidation by (Gibson et al., 1967);

(a) The system of soil is homogeneous.

(b) Both fluid and solid are incompressible.

(c) Hydraulic conductivity and effective stress are only function of void ratio.

As discussed earlier, the relationships between effective stress-pore fluid pressure and excess pore pressure-pore fluid pressure are;

$$\sigma = \sigma' + u_f \tag{3.31}$$

$$u = u_f - u_s \tag{3.32}$$

where u is excess pore fluid pressure,

u_f is pore fluid pressure,

and u_s is static pressure.

Therefore, the gradient of excess pore pressure is

$$\frac{\partial u}{\partial \xi} = \frac{\partial u_f}{\partial \xi} - \rho_f \tag{3.33}$$

by substituting equation 4.6 into 3.30:

$$n(v_f - v_s) = \frac{k}{\rho_f}(\frac{\partial u_f}{\partial \xi} - \rho_f) \tag{3.34}$$

and change it to Reduced coordinates

$$\left[\frac{e(v_f - v_s)}{k\,(1+e)} + 1\right](1+e) + \frac{1}{\rho_f}\frac{\partial u_f}{\partial z} = 0 \tag{3.35}$$

By considering the assumptions and combining the equations 3.24, 3.25, and 3.35, the governing equation for one-dimensional consolidation of soil results in

$$\pm\left(\frac{\rho_s}{\rho_f} - 1\right)\frac{d}{de}\left[\frac{k\,(e)}{1+e}\right]\frac{\partial e}{\partial z} + \frac{\partial}{\partial z}\left[\frac{k\,(e)}{\rho_f(1+e)}\frac{\partial \sigma'}{\partial e}\frac{\partial e}{\partial z}\right] + \frac{\partial e}{\partial t} = 0 \tag{3.36}$$

The first term in equation 3.36 represents effect of self-weight consolidation. Been (1980) showed that this equation reduces to Kynch's theory of sedimentation by setting effective stress to zero. Equation 3.36 is highly nonlinear, and it is applicable for settlement of saturated MFT. Numerical solution for equation 3.36 is discussed in following chapter.

This work focuses on simulation of consolidation for both saturated and unsaturated (gassy) MFT. Gas bubbles are generated by microorganisms through process of bio-densification in MFT. These gas bubbles stay in MFT and make it unsaturated slurry. In following part, equation of consolidation for unsaturated soil is discussed.

3.4 Consolidation of unsaturated slurry

As discussed earlier, gas bubbles are produced by bacteria in biological-activated tailings, and the process of consolidation is called bio-densification. Settlement of gassy slurries is studied in this section to understand effects of gas production in parameters of consolidation.

Understanding settling behaviour of unsaturated slurry is always an issue for soil engineers due to the compressibility of undissolved gas in the system. There are three main sources of gas generation in slurries that are described by Wichman (1999);

a) Biogenic gas, which is produced by bio-degradation of organic matters.

b) Thermogenic gas, which is produced by thermal cracking of complex organic components.

c) Volcanogenic gas, which is produced by geothermal activities happening in

the submarine formation.

Among these sources of gas generation, bio-degradation of organic matters is the dominant source for presence of gas bubbles in oil sands tailings. Undissolved biogenic gas bubbles are connecting and result in trapped gas voids in the tailing. These gas voids are mostly methane and carbon dioxide.

According to Wichman (1999), there are different forms of gas bubbles in the slurry depending on the gas content. (a) Inter-connected voids (b) discrete large bubbles with solid-gas and water-gas interfaces (c) small spheres which are completely surrounded by water in the void (d) dissolved gas in pore water.

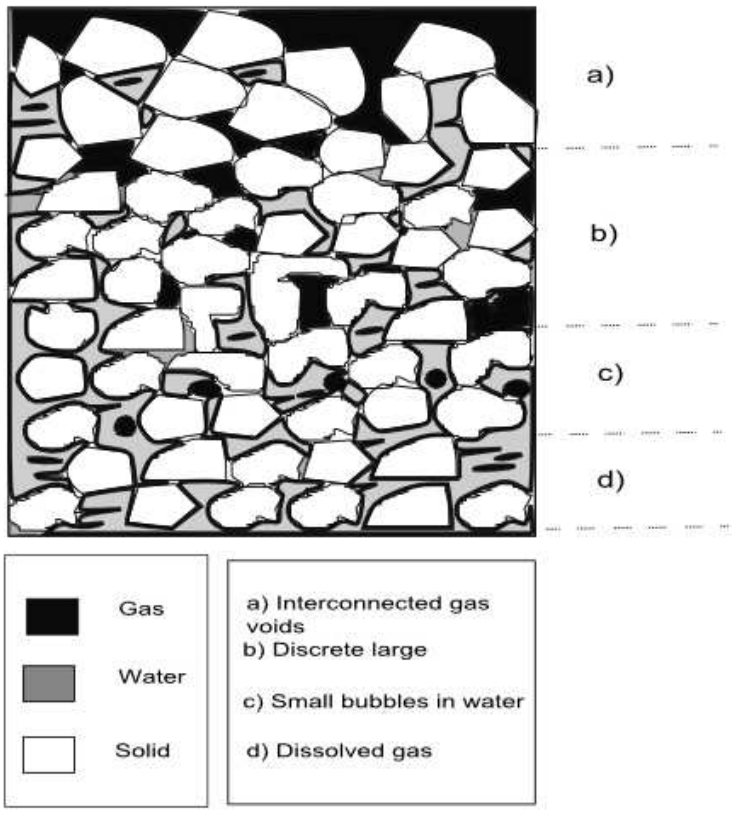

Figure 3.8: Different forms of gas in the unsaturated system (adapted from Wichman (1999))

3.4.1 Review of studies on unsaturated sediments

Extensive studies have been done on characteristics of gassy (unsaturated) soil by Nageswaran (1983), Thomas (1987), Wheeler (1986), Wichman (1999), and Sills and Gonzalez (2001). Most of the current researches are focusing on developing a comprehensive model for gassy soils.

Research on the consolidation behaviour of unsaturated soil started at Oxford in 1978 by Dr. Sills and her research group. They conducted a series of field experiments on measurement of pore water pressure in different locations in saturated and unsaturated soils. They observed that any increase in hydrostatic pressure causes equal increase in pore water pressure for saturated sediment; however exerted pressure differed from final increment in pore water pressure for unsaturated case. They concluded that the compressibility of pore gas causes this reduction in total stress. Their results demonstrated the importance of gas bubbles in geotechnical properties of soil.

Nageswaran (1983) studied effects of gas bubbles in sediments by developing a technique to prepare soil samples with uniform and repeatable distribution of gas bubbles, "zeolite molecular sieve technique" . He applied zeolite powder and methane to simulate the condition in gassy soils. Zeolite consists of interconnecting pores, and has strong affinity for absorbing polar molecules such as water in its pores. Absorbed water can be driven off from pores by heating without changing crystalline shape due to the special characteristic of zeolite. He used the following procedure to prepare gassy soil; Water was dried out from zeolite pores by heating. Then, zeolite was pressurized by methane, and final powder was mixed with soil slurry. Methane gradually replaced by water and was released in soil. As a result, gas voids rose through the soil medium.

The advantages of this method are repeatability and uniformity of conditions. However, the rate of gas production at initial stages is more than rate of self weight consolidation in synthesized gassy soil, which differs from the natural gassy soil.

To overcome this problem, Sills and Gonzalez (2001) conducted a series of experiments to investigate properties of gassy soil. They increased temperature in the sample to fasten the activity of methanogens, and as a result, increased rate of gas production and reduced required time for experiment. Nageswaran also developed an oedometer to measure some properties for gassy soil such as stress and pore-water pressure. The results from oedometer showed that soil with higher initial gas content has higher initial rate of settlement. Also, higher gas content causes lower pore-water pressure increment by increase in applied stress. He proposed that the compressible pore fluid causes the difference between increment in total stress and pore water pressure in gassy soil. He also studied permeability of fluid through soil by gas content and suggested that for slurry with saturation (volume of water/volume of void) of 85 % or more, gas bubbles do not affect the permeability. Because there are only small bubbles at this rate of saturation that are carried by water; however for saturation lower than 85 %, bubbles are interconnected and their permeability become larger than water permeability.

In addition to his experimental efforts, Nageswaran developed a theoretical model based on the Gibson et al. (1967) theory for saturated soil. He assumed water and gas as a compressible and homogeneous pore fluid in the slurry. His model matched the experimental observations for initial consolidation, however failed to predict consolidation behaviour close to the end of the process.

Wheeler (1986) studied undrained shear strength of gassy sediment by a series

of experiments on gassy samples that were prepared by zeolite molecular sieve technique. He also tried to find mathematical formulation for all his experimental results. He considered solid and water as saturated soil matrix that surrounds gas voids. He assumed soil as elastic medium and used mathematical formulation for elastic behaviour of composite material consisting spherical inclusions derived by Hill (1965) to present shear strength of gassy soil.

Thomas (1987) studied the consolidation process of each phases in a gassy soil and tried to obtain relationship between the soil properties, such as stress and pore-water pressure. He used the zeolite molecular sieve technique to prepare gassy samples. He also modified the oedometer for gassy samples that was initially developed by Nageswaran (1983).

Wichman (1999) developed a finite strain consolidation model based on Gibson et al. (1967)'s theory. He considered stagnant gas bubbles in the system. According to his experimental observations, rate of consolidation was decreased by presence of these gas bubbles. He proposed two mechanisms for reduction in rate of consolidation in this system; reduction in specific gravity of soil skeleton because of gas bubbles, and increase in the length of drainage path for water for consolidation. Wichman's theory is used in this work to study effects of stagnant gas voids in unsaturated MFT.

3.4.1.1 Consolidation parameters in unsaturated system

Presence of gas bubbles changes different geotechnical parameters in soil system including consolidation parameters. According to Terzaghi (1936) definition, effective stress is defined as difference between total stress and pore-water pressure. However, this definition is only applicable for incompressible soil. Gas bubbles present in pore fluid make fluid compressible and cause volume

change during water drainage. Therefore, in presence of gas bubbles, the difference between total stress and pore-water pressure is called "operative stress" instead of effective stress. Bishop (1959) presented a modification of Terzaghi' s equation for effective stress in unsaturated system.

$$\sigma' = (\sigma - u_a) + \varkappa(u_a - u_w) \tag{3.37}$$

where $\varkappa$ only depends on degree of saturation, S_r (volume of water/volume of void), and u_a is pore-gas pressure.

The value of parameter $\varkappa$ is defined by degree of saturation, S_r;

$$\varkappa = 1 \qquad s = 100\% \tag{3.38}$$

$$\varkappa = 0 \qquad s = 0\% \tag{3.39}$$

Bishop (1959) conducted a series of experiments to validate equation 3.37, and measured values of $\varkappa$ for samples with different saturation degree.

Sills et al. (1991) defined new operative stress as $\sigma_{op} = \sigma - u$ for large gas bubbles in the sediment. They proposed that the operative stress is only a function of water void ratio in unsaturated soil and it does not depend on gas content of sample. They conducted a series of experiments by preparing samples with different gas contents, measured operative stress, and concluded that operative stress is only a function of water void ratio for soils with large (compared to the soil particles) gas bubbles. Wichman applied this concept in his theory of consolidation for gassy system.

3.4.1.2 Finite strain theory for unsaturated system

These modifications for unsaturated soil are only applicable for gas bubbles trapped in system and does not include gas movement in the soil. Gas bubbles remain in the system when gas content is below a critical value which depends on characteristics of soil. Modifications are based on Wichman (1999) study. He divided unsaturated soil to two parts; compressible (gas voids) and incompressible (saturated soil). He described behaviour of gassy soil under an external force as following; Pore fluid in the system cannot be released in a short time after acting the force. Therefore, fluid void ratio remains constant, $e_f = \frac{V_f}{V_s}$. However, gas bubbles are compressed by this external force. As a result, degree of saturation increases, and total void ratio will decrease which indicates $c_f = S_r e$ is constant in the system. S_r is degree of saturation and is defined as $\frac{V_f}{V_{void}}$. As pore fluid does not flow out of the system, increase in total stress directly converts to excess pore pressure in fluid. Hence, operative stress $\sigma_{op} = \sigma - u_f$ and fluid void ratio remain constant. Wichman concluded that the operative stress which acts in unsaturated soil is similar to effective stress in saturated soil, and it is only controlled by fluid void ratio. Fluid void ratio is defined in terms of degree of saturation and porosity as $e_f = \frac{S_r n}{1-n}$.

Wichman (1999) modified one dimensional finite strain consolidation of saturated soil by Gibson et al. (1967) according to following concepts. Through process of consolidation, water flows out of solid structure, and released water accumulates on top of sediment. As gas voids are connected to solid skeleton, gas voids are compressed when solid particles settle down (Figure 3.9). Increase in gas pressure due to compression causes dissolution of gas in pore water according to Henry's law. Solid interface changes with time due to compression, dissolution of gas voids, and water removal.

Therefore, it is formulated based on Reduced coordinate as

$$z(\xi, t) = \int_0^{\xi} \frac{d\xi'}{(1 + e_f(\xi', t) + e_g(\xi', t))} \tag{3.40}$$

where ξ is Convective coordinate, e_g is gas void ratio ($\frac{Gas\,Volume}{Solid\,Volume}$), and z is Reduced coordinate.

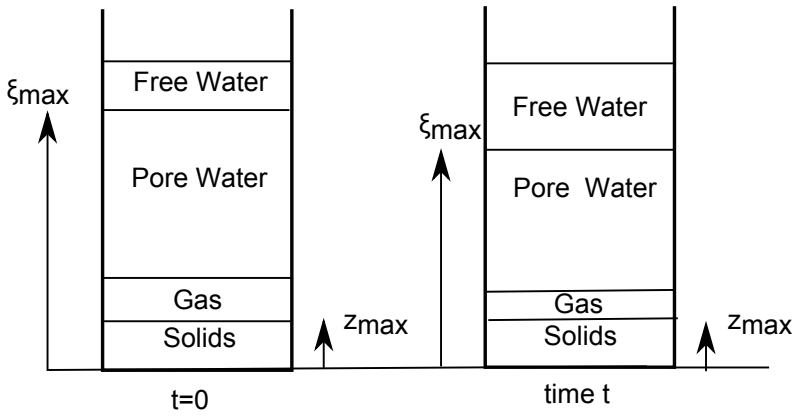

Figure 3.9: Consolidation of gassy soil (relation of Convective and Reduced coordinates) modified from Wichman (1999)

Total stress and flow discharge are defined in terms of void ratio and height to derive final governing equation. Total stress at point z is summation of three terms; weight of solid and water on that point, free water, and load.

$$\sigma = \int_z^{z_{max}} (\gamma_s + e_f(z', t)\gamma_f)dz' + \gamma_f(h_{water} - \xi_{max}(z_{max}, t)) + load \tag{3.41}$$

where z_{max} is total solid height.

The fluid discharge is defined as change in volume of pore fluid in the system

$$q = -\int_0^{z} \frac{\partial}{\partial t} e_f(z', t)dz' \tag{3.42}$$

Bottom is impervious thus there is not any discharge from the bottom.

For the saturated part of soil Darcy's equation for movement of pore fluid in soil skeleton is used;

$$q = -\frac{k}{\gamma_f}\frac{\partial u}{\partial \xi} \tag{3.43}$$

By substituting $\frac{\partial u}{\partial \xi} = \frac{\partial}{\partial \xi}(u_w - \gamma_f(\xi_{max} - \xi))$ and $\frac{\partial}{\partial \xi} = \frac{1}{(1+e_f+e_g)}\frac{\partial}{\partial z}$, Darcy's equation changes to;

$$q = -\frac{k}{\gamma_f}\frac{1}{(1+e_f(z,t)+e_g(z,t))}\frac{\partial u_w}{\partial z} - k \tag{3.44}$$

where k is coefficient of permeability, u_w is pore-water pressure, and u is excess pore water pressure.

Equations 3.40 to 3.44 are used to obtain the finite strain theory of consolidation for unsaturated system;

$$\begin{aligned}\frac{\partial e_f}{\partial t} = &-\frac{\partial e_f}{\partial z}\frac{\partial}{\partial e_f}\left[\frac{k(e_f)}{\gamma_f(1+e_f+e_g)}\left\{(\gamma_s - \gamma_f(1+e_g)) + \frac{\partial \sigma_{op}(e_f)}{\partial z}\right\}\right] \\ &+ \frac{\frac{\partial e_g}{\partial z}}{(1+e_f+e_g)^2}\frac{k(e_f)}{\gamma_f}\left[(\gamma_s + \gamma_f e_f) + \frac{\partial \sigma_{op}(e_f)}{\partial z}\right]\end{aligned} \tag{3.45}$$

By assuming that the gas voids are uniformly distributed in different heights, i.e. $\frac{\partial e_g}{\partial z} = 0$, in equation 3.45;

$$\begin{aligned}\frac{\partial e_f}{\partial t} = &-\left\{\frac{(\gamma_s - \gamma_f(1+e_g))}{\gamma_f}\right\}\frac{\partial e_f}{\partial z}\frac{\partial}{\partial e_f}\left[\frac{k(e_f)}{(1+e_f+e_g)}\right] \\ &- \frac{\partial}{\partial z}\left\{\frac{k(e_f)}{\gamma_f(1+e_f+e_g)}\frac{\partial e_f}{\partial z}\frac{\partial \sigma_{op}(e_f)}{\partial e_f}\right\}\end{aligned} \tag{3.46}$$

If we substitute $e_g = 0$ in equation 3.46, it turns into the finite strain theory of consolidation for saturated soil. Finite strain equation of consolidation for

gassy system is solved in chapter 5 to predict rate of settlement in unsaturated MFT.

Chapter 4

Experimental Observations

Experiments were conducted to investigate effects of different parameters including coefficients of consolidation, gas production, and ion concentration in settling characteristics of MFT. Also, results of these experiments are used to verify developed models. The procedures and results of these experiments are discussed in this chapter.

4.1 Settling columns (2 m)

Two columns (Figure 4.1) were installed to investigate settling characteristics of unamended (original) and amended (the one with addition of Canola waste) MFT. Syncrude MFT is used to prepare samples of columns, which contains 36 % solids, 61 % water, and 2.5 % bitumen. This MFT was diluted to 25 $wt\%$ by adding cap water to original sample. To avoid aeration in the sample, water was mixed with MFT under N_2. Two columns were filled with 46 L of 25 % MFT; one with only MFT (unamended), and the other with MFT mixed by canola (amended). Canola (72.3 g) was mixed with MFT (30 L) under N_2 to

prepare amended sample. Final samples were transferred to the columns and sealed with silicon glue. Gas trap was installed on the top of the columns to measure volume of released gas from the samples in each column. Early in experiment, gas bubbles were produced in the amended column and released in gas trap. However, there was no evidence of gas release in unamended column.

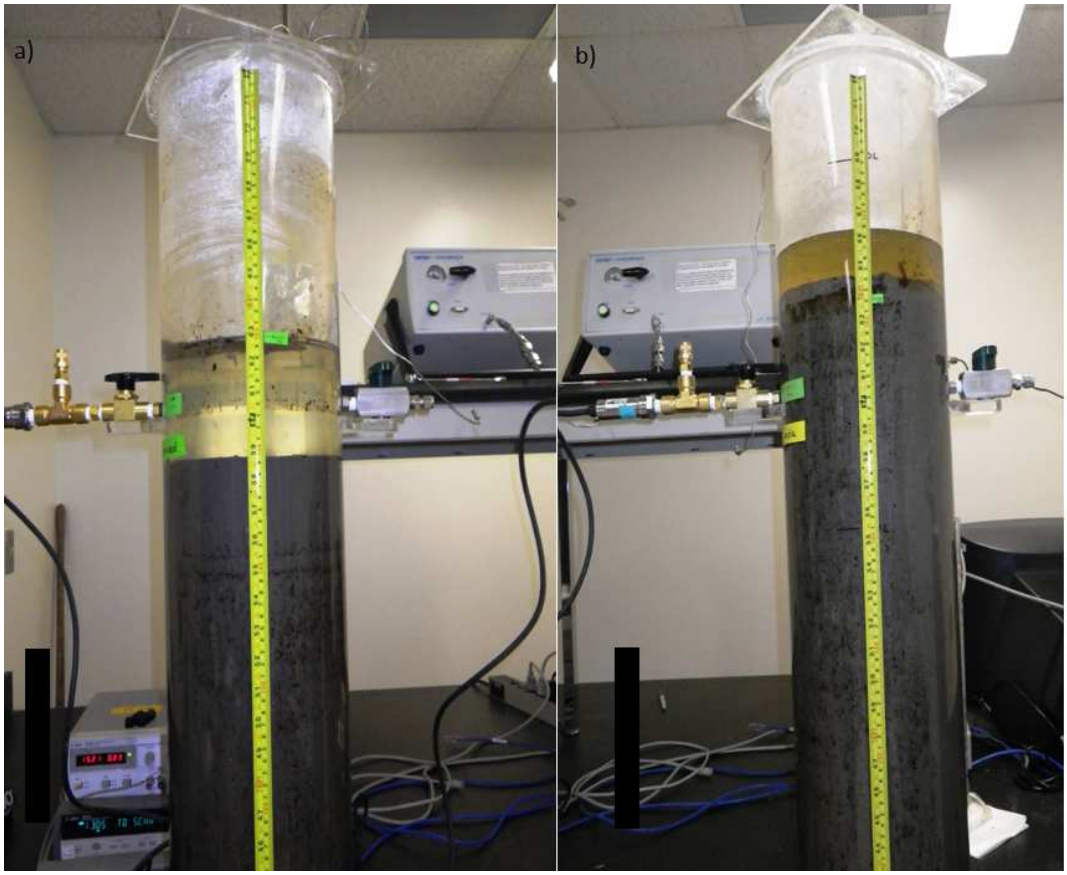

Figure 4.1: $2\,m$ columns at University of Alberta a) Unamended MFT b) Amended MFT (courtesy to Rozlyn Young)

Pore-water pressure is measured in three different ports in columns for better understanding of their settling characteristics. Results of solid interface and released water for 144 days illustrated in Figures (4.6 and 4.3). In gassy MFT (amended) column, solid interface gradually rose in first 55 days of process due to accumulation of trapped gas in system. After the initial increase in height,

the solid interface dropped dramatically and substantial volume of water was released. This phenomenon could be explained by collapse of gas bubbles due to increase in pressure of their surrounding environment. Two hypotheses are proposed to describe sudden increase in volume of released water right after collapse of system. First, gas cracks produced by connection of gas bubbles create drainage path for water, and increase consolidation rate in gassy MFT. Also, diameter of gas bubbles increases due to pressure difference between inside and outside of bubbles that compress surrounded soil skeleton and accelerate rate of water release. In unamended MFT, solid settles down slowly without any increase in height. The final solid interface of both samples are almost the same after 140 days, however there is a big difference in volume of released water in these samples. These data are used to verify model prediction for coefficients of consolidation.

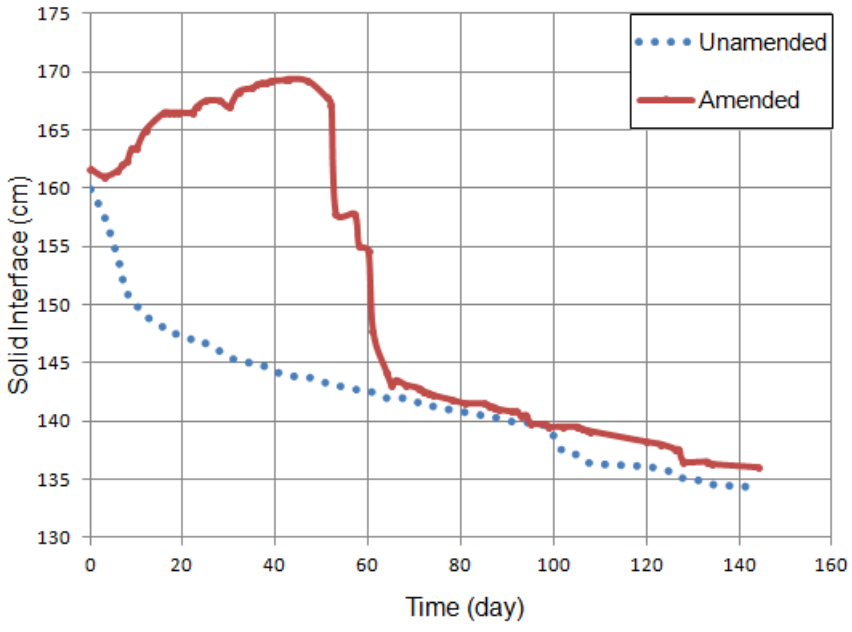

Figure 4.2: Solid interface for both amended and unamended columns

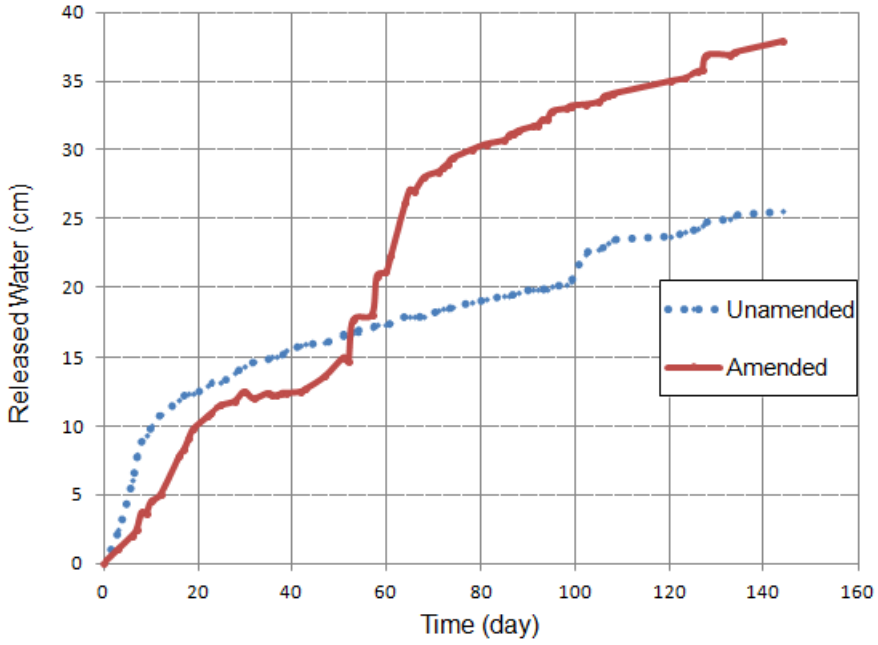

Figure 4.3: Released water for both amended and unamended columns

Pore-water pressure is measured in three different ports in amended column and results illustrated in Figure 4.4. There is a sudden drop in pore-water pressure after about 48 days in all ports. This pressure drop happens during of sediment collapse. It is observed that MFT consolidates dramatically and water is expelled out at the time of collapse. Due to this dramatic change, pore-water pressure drops down suddenly for few days and rises up again after system stabilized.

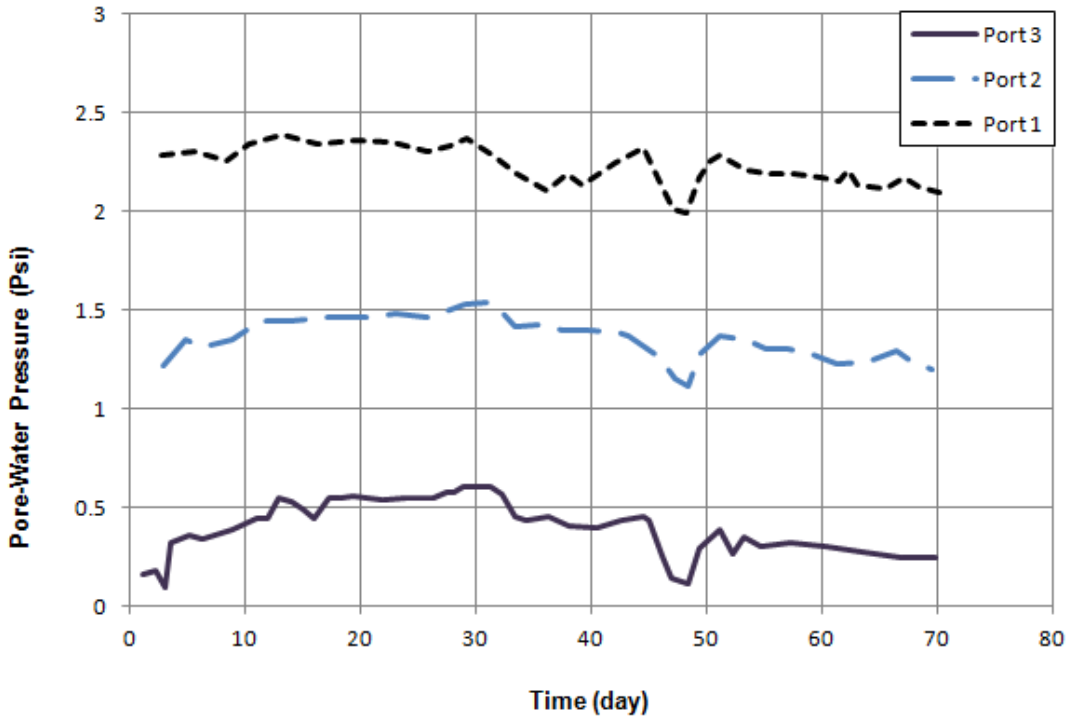

Figure 4.4: Pore-water pressure in three different ports in amended column

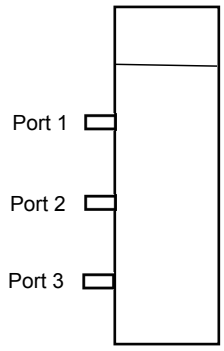

Figure 4.5: Pressure transducers at three different locations

4.2 Preparation of bitumen-free MFT

MFT is a complex mixture of water, solid and organic matters, which makes it difficult to investigate effects of individual parameters in its settling rate. Therefore, a synthesized MFT was prepared in laboratory to investigate effect of ion concentration in rate of consolidation. The procedure is described in following parts.

4.2.1 Centrifugal method of separation

Centrifugal technique is used to separate bitumen from MFT. This technique is common for fast separation of particles or fluid from slurries.

The settling rate of solid particles in a gravity field is related to different parameters such as particle size, difference between solid and liquid density, and viscosity of suspension. Settling of solid particles in MFT is very slow; therefore centrifugal force is used to reduce the required time for settlement. The settling velocity of particles under centrifugal force is calculated according to Stokes law.

$$u_c = \frac{(\rho_p - \rho_f)}{18\mu}.r\omega^2 \tag{4.1}$$

Where ρ_p and ρ_f are densities of particle and surrounding medium, d_p is particle diameter, μ is viscosity of the suspension, r is distance from center of rotation, and ω is the angular velocity. There is a relation between centrifugation speed (RPM) and angular velocity:

$$\omega = \frac{2\pi n}{60} \tag{4.2}$$

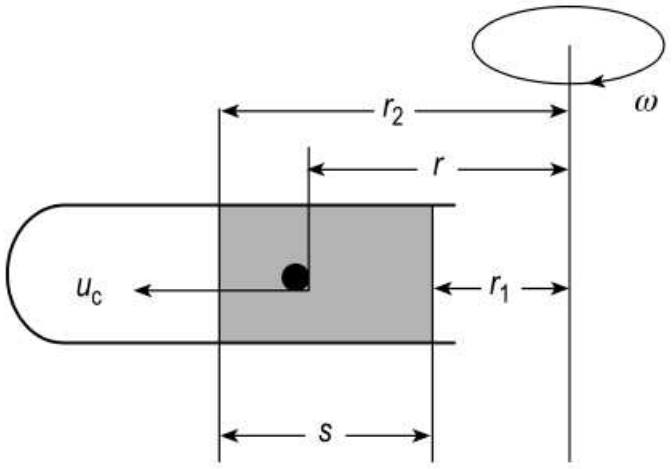

Figure 4.6: The schematic picture of particle settling during centrifugation

The practical way to measure the settling velocity of particle is to calculate the movement of particle in the bottle. As illustrated in Figure 4.6, the following equation can describe particle motion in the bottle:

$$u_c = \frac{dr}{dt} \tag{4.3}$$

u_c is velocity under gravitational force, therefore it is converted to velocity under centrifugal force with

$$u_c = u_g \frac{r\omega^2}{g} \tag{4.4}$$

where g is acceleration due to gravity and u_g is velocity under gravity.

Particles should move to a radius bigger than r_2 in Figure 4.2 to settle. Particles on the surface of liquid will move the longest path, start from r_1 to a radius bigger than r_2.

By rearranging and combining equations 4.3 and 4.4, required time for settling of particles is

$$\int_0^T dt = \frac{g}{\omega^2 u_g} \int_{r_2}^{r_1} \frac{dr}{r} \tag{4.5}$$

$$T = \frac{g}{u_g \omega^2}.ln\frac{r_2}{r_1} \tag{4.6}$$

Where T is the spinning time required for all particles to move from r_1 to r_2 and settle. By replacing the velocity of particles from Stokes law in equation 4.6, settling time for particles under centrifugal force is

$$T = \frac{18\mu}{d^2\left(\rho_p - \rho_f\right)\omega^2(1-\phi_f)^n}.ln\frac{r_2}{r_1} \tag{4.7}$$

where ϕ_f is the solid volume concentration, μ viscosity of fluid, ρ_p is the density of sphere, ρ_f density of fluid. Equation 4.7 is used to calculate required time for centrifugation in which all particles in MFT settle down.

4.2.2 Separation of bitumen from oil sands tailings

To provide same solid distribution of particles as MFT, bitumen is removed from the sample at initial step. Mature fine tailings with 25 $wt\%$ solid content is provided by Syncrude Canada. Separation procedure consists of two steps; pre-treatment of MFT and bitumen separation using toluene.

Water and toluene are immiscible; therefore pore-water in MFT prevents toluene to separate bitumen from slurry. Water should be separated from slurry prior to bitumen removal. This step is called pretreatment and to fasten process of separation Sorvall RC-5B Superspeed centrifuge is used. Around

$200\,g$ MFT (25 %) is weighted and centrifuged in the $250\,ml$ FEP centrifuge bottles with Tefzel screw closure. The sample is centrifuged for 2 hours and 11 minutes with speed of 6000 RPM. The required settling time is calculated according to equation 4.7.

After removing pore water from MFT, bitumen is separated from the treated sample. About $50\,g$ of separated solid is placed in the $250\,ml$ FEP centrifuge bottles with Tefzel screw closure, and about $200\,ml$ toluene is added to each bottle. To disperse the solid in toluene, the sample is placed in a reciprocating shaker for $1\,hr$. Once samples are dispersed in toluene, they are placed in the same centrifuge as previous step for $1\,hr$ and $45\,min$ with $6000\,RPM$ in $4°C$. After centrifugation, separated bitumen and toluene are discarded. About $200\,ml$ toluene is added to the solid for removal of remaining bitumen. This procedure is repeated until all bitumen is removed. Complete removal of bitumen is recognizable by observing clear toluene after centrifuging. After separation of bitumen, solid particles are washed and dried for complete removal of toluene. In the next step, organic matter is removed from the tailings.

4.2.3 Separation of organic matter from oil sands tailings

The dried soils are placed in a $2\,L$ beaker, and water is added about $20\,ml$ per $10\,g$ of sample. The beaker is placed in a water bath with the constant temperature of $70°C$. Hydrogen peroxide (30 %) is added to the beaker ($1\,\frac{ml}{g}$ of solid). Due to reaction of hydrogen peroxide with organic matters, sample starts frothing. Acetic acid can be used to stop frothing of sample, one drop at a time. After frothing stopped, more hydrogen peroxide is added to the sample in the same amount as before ($1\,\frac{ml}{g}$ of solid). The end of reaction is when the

froth formation stops in the beaker, this time more hydrogen peroxide is added to beaker ($1\,\frac{ml}{g}$ of solid) to ensure consumption of all organic matters. The beaker is placed in the water bath for $3\,hr$ for decomposition of all unused hydrogen peroxide by heat. The treated sample then is centrifuged for water separation. Sample is washed and centrifuged to get colorless supernatant.

The solid is dried in oven, and this dried solid has the same clay and fine distribution of initial MFT. Also, it is free of bitumen and organic matter and simpler to study. The particle size distribution is determined for the final synthetic solids in next part.

4.2.4 Particle size distribution

Particle size distribution of MFT is an important parameter in prediction of its settling behaviour. To begin the analysis, the particles are dispersed to avoid particle aggregation in the solution. After dispersion of particles, the size distribution of particles is calculated based on measuring physical characteristics of suspended particles. Around $5\,g$ of synthesized MFT is dispersed in water and its particle size distribution is measured by Malvern Mastersizer 2000 . Results are illustrated Figure 4.7.

Two main fractions are defined to describe distribution of soil particles: fine particles (clay, silts and sands with diameter less than $2\,mm$) and coarse particles (stones with particle size more than $2\,mm$). The fine particles are divided into three different size fractions (clay fraction less than $2\,\mu m$, silt fraction between 2 and $20\,\mu m$, and sand fraction 0.02 to $2\,mm$).

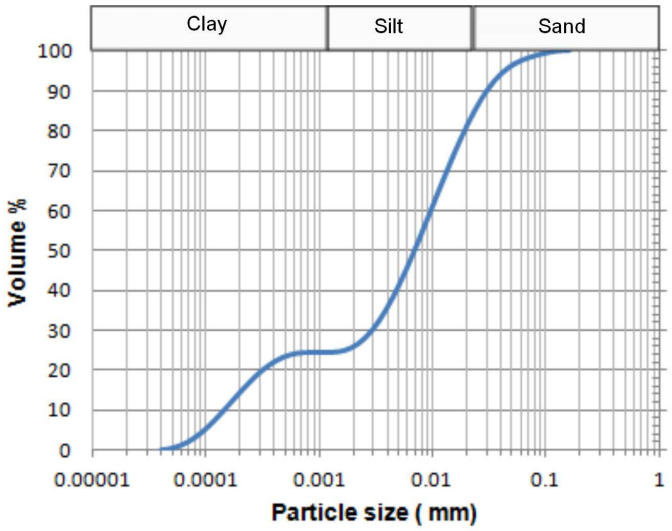

Figure 4.7: Particle size distribution for synthetic fine particles

Consolidation of MFT takes a long time, therefore it is common to use consolidation test to predict magnitude of settling rate. In next part, this test is described in detail.

4.3 Consolidation test

Finite strain theory is used to predict the settling rate of tailings in the $2\,m$ columns as described in part (4.1). To solve equation of finite strain, it is essential to calculate consolidation parameters including compressibility and permeability. Compressibility is relationship of effective stress with void ratio and permeability correlates hydraulic conductivity with void ratio. Consolidation parameters are varying for different tailings, and are measured by an apparatus called consolidometer. Consolidation tests are performed to estimate compressibility and permeability of confined soil material based on large strain equations by Terzaghi. In calculation of compressibility, it is more con-

venient to use effective stress as the independent variable and calculate the void ratio.

There are different procedures for measuring consolidation parameters. Znidarcic et al. (1984) summarized practical consolidation tests that are using the same form of governing equations as step loading, constant rate of deformation, controlled gradient, constant rate of loading, continuous loading, seepage and relaxation test. These tests are different in initial, boundary conditions and procedure for calculation of parameters. The step loading test is used in this project thus it is described in following part.

4.3.1 Consolidometer

The concept of consolidometer originates from the standard oedometer which uses step loading procedure. In the step loading test, loads are applied on a thin specimen gradually and consolidation properties are calculated through the process. In first step, material consolidates under its own weight without any load. The completion of each step is determined by dissipation of excess pore-water pressure. This test requires several weeks to several months to be completed, which could be considered as the main disadvantage of this method.

The standard oedometer is only suitable for material with small strain during consolidation. However, mature fine tailing (MFT) is slurry with high initial water content and its volume changes dramatically under consolidation. Therefore, standard oedometer is not a proper option for measuring consolidation parameters. A modified step-loading apparatus was built at University of Alberta, Geotechnical Centre, to overcome this problem. Jeeravipoolvarn (2005) described the equipment and the test procedure.

The concept of the equipment is the same as standard oedometer, loads are added to the sample in each step according to the properties of sample in that stage. Each step finishes when the excess pore-water pressure, which was produced due to extra load, dissipates. The hydraulic conductivity test, for measuring permeability, is run between two steps.

To calculate consolidation properties of synthetic MFT, two modified oedometers are designed based on description by Jeeravipoolvarn (2005) and built at Chemical Engineering Department, University of Alberta (Figure 4.4) .

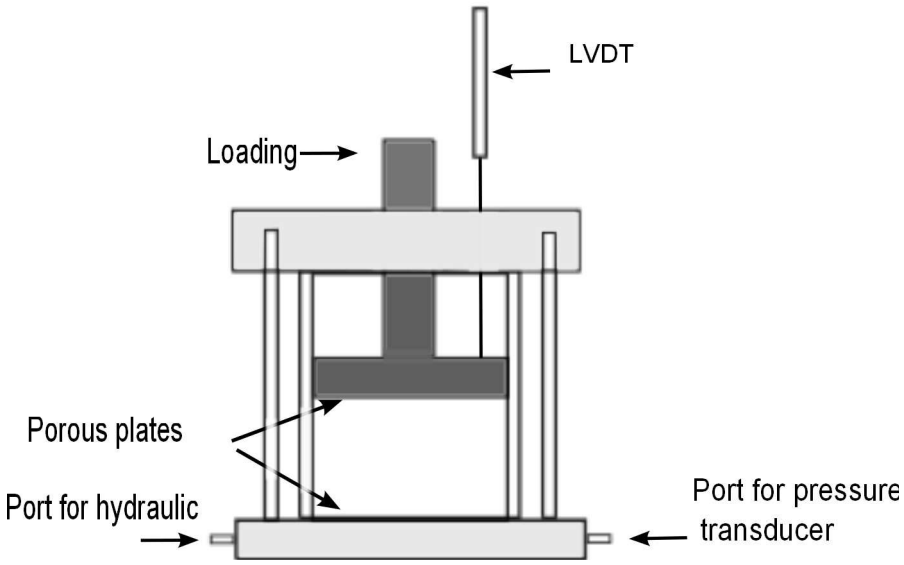

Figure 4.8: Schematic picture of consolidometer

4.3.2 Hydraulic conductivity test

There are different methods for measuring hydraulic conductivity; however few of them are explained in this work. All methods are divided into two main categories; direct and indirect.

4.3.2.1 Indirect method

In the indirect method, hydraulic conductivity is determined by applying equations of consolidation on data generated from consolidation test. There are different tests in this category such as step loading, controlled gradient, constant rate of deformation, and constant rate of loading test. In the most common indirect methods, permeability is determined by inverting Terzaghi's theory. However, the constant permeability and compressibility that are assumed in Terzaghi's theory make this method unsuitable for compressible natural clays (Suthaker, 1995). Therefore, in this study direct method is used for measurement of hydraulic conductivity as the sample is highly compressible.

4.3.2.2 Direct method

In this method fluid is forced through the specimen and its flow rate is measured. Based on flow rate of fluid through sample and hydraulic gradient, hydraulic conductivity is calculated.

Constant and falling head tests Two common methods for direct measurement of hydraulic conductivity are constant head and falling head. In the constant head test, fluid goes through the sample due to constant head gradient that is forced on system. Constant head test is more accurate for granular samples where flow rate is high. However, for fine grained soil, falling head test is more proper in which the gradient is changing constantly. In both methods, flow rate is measured to calculate hydraulic conductivity.

There are some disadvantages associated with these methods, which are discussed by Olsen et al. (1985). One of the main disadvantages is accuracy

of measurement. Flow rates in these methods are calculated by measuring changes in fluid volume. As volume is measured by conventional methods, maximum resolution is in order of $10^{-3}\,ml$. Therefore, for calculating hydraulic conductivity of samples with low permeability, higher gradient is required to enable volume measurement. Increase in hydraulic gradient changes effective stress, and as a result permeability of sample. Therefore, calculated hydraulic conductivity is not reliable. Another problem with falling test is constant changes in gradient which changes effective stress and permeability of sample. Several modified tests such as automatic head permeameter test and rising tail water test have been introduced to solve these problems. These tests are all following the same principle as falling head test but they provide more reliable results (Daniel, 1989; Tan, 1989).

Flow pump test This test first was proposed by Olsen et al. (1985) for measuring permeability of fine grained soil. In this method, a constant flow is forced into the sample by a pump. The exerted gradient is calculated by measuring pressure with differential pressure transducers. Aiban and Znidarcic (1989) reported that the results of this test are similar to results of constant head test under the same test condition.

Restricted flow test In this method, the total stress is applied to one side of sample and drainage is allowed only from another side through a restrictor. Pore-water pressures at two sides are measured, and hydraulic gradient is calculated from pore-water pressure gradient and sample height. One of the challenges of this method is accurate measurement of pore pressure. At the beginning of this test, pressures are large and the pressure transducer for measuring those is not suitable for measuring small differences in pres-

sure. Differential pressure transducer could be used to overcome this problem (Suthaker, 1995).

Seepage test In this test, flow is forced through the sample by application of constant head and pore pressure distribution is measured through the sample. The test continues until pore pressure distribution reaches a steady state condition. After completion of test, sample is sliced for calculating void ratio distribution. Hydraulic gradient is calculated from pore-water distribution, and void ratio-permeability relation is obtained with measuring flow rate and void ratio distribution.

The combination of step loading consolidometer with constant head permeability test is used for measuring consolidation parameters of saturated slurry in this study. As we are dealing with unsaturated MFT, consolidometer for gassy slurry is discussed in following part.

4.3.3 Consolidometer for gassy slurry

To solve the equation of consolidation for gassy soil, calculation of consolidation parameters is essential. However, the regular oedometer cannot be used for gassy soil. Nageswaran (1983) developed a special oedometer, which allowed the consolidation of gassy system. The first set-up was developed at Oxford University with following capabilities;

a) Measuring coefficient of consolidation, effective stress, and pore-water pressure for very soft gassy soil.

b) Separation of free gas from drained pore fluid.

c) Measuring total vertical stress on soil sample and pore-water pressure on undrained side.

d) Measuring volume of each phase (solid, gas, water) during consolidation process.

In the test, load increases instantaneously with the constant rate up to a maximum value. The equipment allows the measurement of total volume of sample, volume of water draining from the sample, and as a result changes of gas volume in sample. The load was exerted by hydraulically activated piston applied on the top of piston. Drainage of gas and water during consolidation are only through the top part where gas and water are separated. The important parameters such as vertical total stress, pore-water pressure at the top and bottom of cell are recorded.

To describe the stress-strain behaviour of saturated soil, effective stress should be related to void ratio. However, in the gassy soil the difference between total stress and pore-water pressure is called operative stress (Sills and Gonzalez, 2001). Therefore, stress-strain behaviour of gassy slurry is determined by operative stress and water void ratio. This relationship is equated in following form (Wichman, 1999)

$$\sigma_{op}(e_f) = \sigma_0 exp(m_1 + m_2 e_f) \tag{4.8}$$

where e_f is fluid void ratio, and m_1 and m_2 are constant parameters and are changing for different soil samples.

Permeability of gassy soil is calculated from measuring the pore water discharge, pressure gradient and use of Darcy's law. In gassy slurry, permeability and void ratio are related in the form of (Wichman, 1999)

$$k(e_f) = k_0 exp(m_3 + m_4 e_f) \tag{4.9}$$

The equation of permeability and operative stress are substituted into equation of consolidation for gassy soil to calculate the rate of settlement. This equation is solved in chapter 5 to predict settling rate of consolidation for gassy slurry.

In the next part, sample preparation and test procedure for calculating coefficients of consolidation are explained.

4.4 Effects of chemical ions in rate of settlement

It is proposed that changes in chemical ion concentration due to microbial activity is one the main reasons for increased rate of consolidation in amended MFT. Experimental results for ion concentration in amended and unamended MFT showed dramatic difference in concentration of bicarbonate (HCO_3^-) and carbonate (CO_3^{-2}) ions in these two samples. Therefore, effect of bicarbonate in settling characteristics of slurry is investigated in this study.

Effects of bicarbonate anions are studied in synthesized MFT to avoid the complexity of original MFT. As described earlier (part 4.2), bitumen and organic matters are separated from MFT. Two series of experiments are conducted; measurement of consolidation parameters and measurement of settling characteristics of synthesized MFT. These studies are explained in following parts.

4.4.1 Consolidation test on synthetic MFT

4.4.1.1 Sample preparation

Two samples are prepared with different concentration of bicarbonate ion. According to chemical analysis of amended and unamended columns, concentration of bicarbonate increases from $\sim 900\,ppm$ to $\sim 1800\ ppm$ due to microbial activity. Therefore, two slurries are prepared with concentration of 900 ppm and 1800 ppm of HCO_3^- .

Nanopure water is mixed with synthesized fine particles to prepare slurry with $25\,wt\%$ solid content. Sodium bicarbonate is selected to control concentration of bicarbonate ions in samples and is added to samples to make the two slurries with desirable concentrations.

Samples are transferred to the consolidometer for measurement of consolidation parameters. Two consolidometers (Figure 4.9) made in Chemical Engineering Department at University of Alberta to measure consolidation parameters of samples.

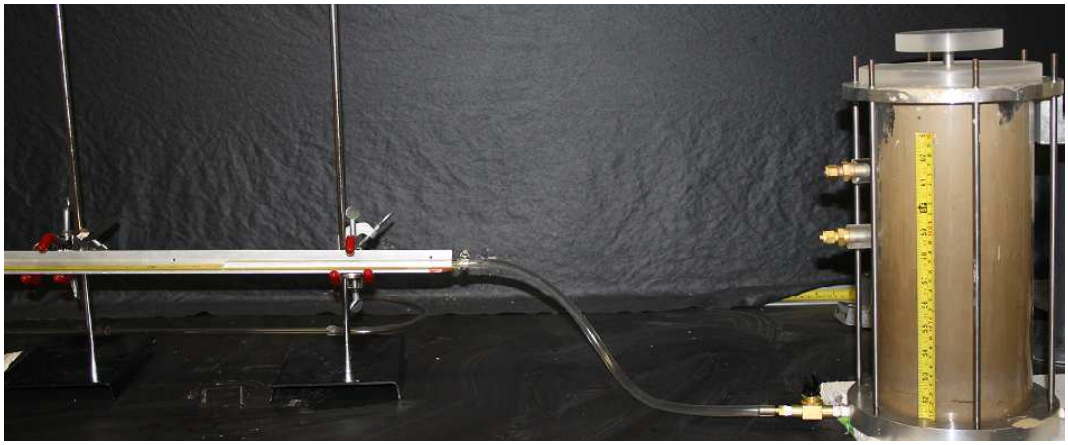

Figure 4.9: Consolidometer and hydraulic conductivity measurement setup

4.4.1.2 Test procedure

The following steps describe the procedure as used in this study (based on procedure by Jeeravipoolvarn (2005)) ;

1. Prepare sample for the test as explained in sample preparation part. Volume of sample depends on the size of equipment especially to its diameter. The ASTM (2004) suggests that diameter of equipment should be at least two times larger than height of sample.

2. Set up the equipment as shown in Figure 4.4 and fill it with the same water in your sample and let base and permeability tube be saturated with water. The outlet tubes should be at the same height as outlet valves.

3. Put one filter paper at the base of equipment and close outlet valve. Make sure that the bottom plate is completely sealed. Fill the cell with the sample.

4. Put another filter paper on top of sample and close top of the cell with the cap. Measure the initial height of sample and record the initial pore-water pressure as measured by a pressure transducer at the bottom of cell.

5. Let the sample self consolidate under its own weight. Monitor the height of sample and pore-water pressure at the bottom regularly and record the data.

6. Let the sample settle completely. Completion of settlement could be understood by dissipation of excess pore-water pressure and observation of solid interface. Excess pore-water pressure becomes zero and dissipates when measured pore water pressure is equal to hydrostatic pressure. Also, at the end of settlement, solid interface becomes constant with time.

7. Record the final interface of solid and pore-water pressure after completion of settlement. Calculate settling stress in the middle of sample based on void ratio at the end of settling process.

8. Conduct the hydraulic conductivity test after completion of settling in each step. The test is explained in next part.

9. Calculate the amount of weight required for settling of sample in next step based on calculated stress in step 7. Take off the cap and put the piston on top of sample. This step should be performed carefully and slowly to prevent agitation of sample. Then, connect the LVDT to the piston rod to measure solid interface precisely. Measure the weight of piston and LDVT bar and subtract them from the required load for settlement of sample. Put load on piston to provide the required weight for settlement. Let the sample settle and monitor the height and pore-water pressure as explained in step 5.

10. Conduct hydraulic conductivity test with constant head after completion of settlement (look at hydraulic conductivity test for more detail).

11. Measure the stress in the middle of sample. Put extra loads on top of sample to double the stress in the middle. After each step, run hydraulic conductivity test and record all data such as solid interface, pore-water pressure, and stresses.

12. Repeat steps 10 and 11. The final load for the test is determined based on nature of sample in cell. Jeeravipoolvarn applied up 1000 kPa on MFT sample to measure consolidation parameters.

13. After loading is finished, unload sample by taking out loads one at a time and reduce stress from final stress to initial stress. At the end of unloading, remove sample layer by layer to calculate water content and void ratio in each layer.

4.4.1.3 Hydraulic conductivity test

According to properties of sample, constant head test was selected to calculate hydraulic conductivity of samples in this study. Small hydraulic gradient is applied on sample and water flow rate through the sample is measured. As illustrated in Figure 4.9, apparatus is built of a long permeable tube with $ID = 7\,mm$ which is connected to consolidometer with hose. A holder is used to keep the tube at constant height and provide constant head for water to go through sample in the cell. The test procedure is explained in following steps;

1. Flush the tube and hose with the fluid that is used in sample preparation.

2. The inlet flow valve should be closed after filling hose and tube with fluid.

3. Open the out flow valve in the middle of the cell and put a beaker to collect outflow fluid.

4. Adjust the tube holder in the height in which forced fluid to flow through the sample without agitation.

5. Open the inflow valve for fluid and start your stopwatch. Measure the flow rate of fluid as it goes through the sample and calculate hydraulic conductivity based on Darcy's equation.

6. Continue the test until the measured hydraulic conductivity is stable.

7. Close the inflow valve, and record the final hydraulic conductivity.

This test as described in consolidometer test should be run after completion of each step.

To calculate consolidation rate of particles in slurry, it is essential to find stress-void ratio and permeability-void ratio relationships for sample. Somogyi (Winnipeg 1980) assumed that there is a power law relationship between

effective stress-void ratio and permeability-void ratio for saturated soil;

$$e = A\sigma'^{B} \tag{4.10}$$

$$k = Ce^{D} \tag{4.11}$$

where e is void ratio, σ' is effective stress, k is coefficient of permeability, and A, B, C, D are constant parameters. These constant parameters are changing for different soil samples, and are measured based on consolidation and permeability tests. These parameters are substituted in chapter 5 and equation of consolidation is solved for saturated MFT.

4.4.2 Settling columns (2 L)

As explained earlier, concentration of chemical ions changes during bio-densification of tailings. To study effect of ion concentration in settling behaviour of bio-activated tailings, four samples are prepared. Solid part of sample is prepared according to procedure in part (4.3) and has the same particle distribution as original MFT. Slurries with 25 $wt\%$ solid content and bicarbonate ion concentration of 0 ppm, 500 ppm, 1000 ppm, and 2000 ppm are prepared (Figure 4.10). Nanopure water, solid and sodium bicarbonate are mixed in order to achieve these anion concentrations. These samples are placed in graduated cylinders to settle.

Figure 4.10: Settling columns with different sodium bicarbonate concentration (initial condition)

Solid interface in all cylinders are measured every day and results are shown in Figure 4.11. Settlement of solid in cylinder without bicarbonate ion was negligible after 15 days; however, solid interface dropped up to 3 cm for sample with 2000 ppm ion concentration. There is substantial differences between volume of released water in these columns as shown in Figures (4.10 and 4.13).

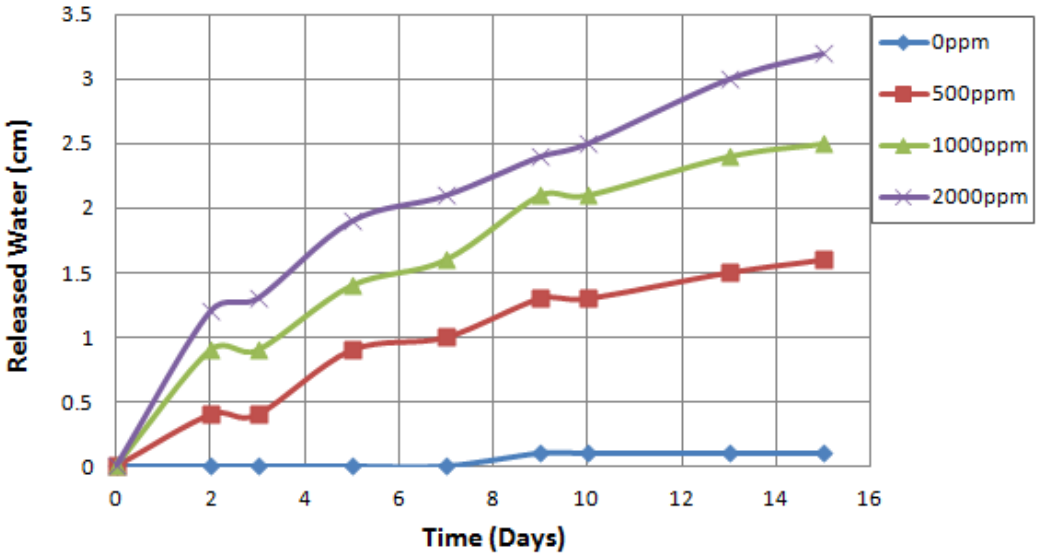

Figure 4.11: Released water for 2 L settling columns

Figure 4.12: Settling columns with different sodium bicarbonate concentration (after 10 days)

Samples are compared from close shot in Figures (4.13 and 4.14) after 10 days.

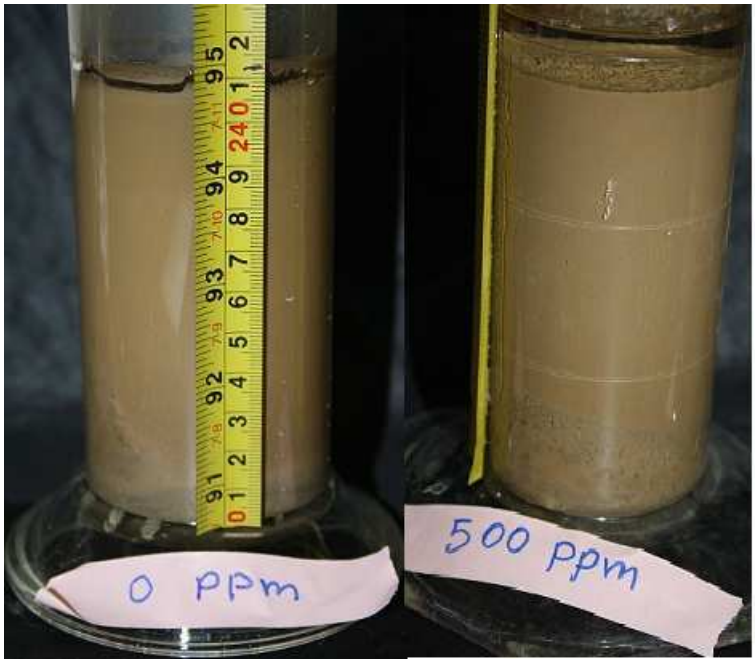

Figure 4.13: Settling columns (without and with 500 ppm $NaHCo_3$) after 10 days

Figure 4.14: Settling columns (1000 ppm and 2000 ppm $NaHCo_3$) after 10 days

Structure of two samples ($0\,ppm$ and $2000\,ppm$) are examined by SEM test to investigate effect of bicarbonate anion on structure of slurry (Figures 4.15 to 4.20). As illustrated in SEM pictures, in sample with bicarbonates solid particles are well structured while they have a loose structure in absence of bicarbonates. Tang (1997) studied effect of bicarbonate on structure of MFT, and proposed that bicarbonate anions and pH are two main factors that cause dispersed (card-house) structure of MFT. She conducted a series of experiments and concluded that MFT with pH values between 8 and 10 has card-house structure. It should be noted that HCO_3^- converts to H_2CO_3 at pH lower than 8 and to CO_3^{-2} at pH higher than 10 and it has the highest concentration at pH values between 8 and 10. Therefore, as she pointed out, the dispersed nature of MFT could be attributed to pH or concentration of HCO_3^-. However, in her study, the main factor has not been distinguished.

In this study, pH values of samples are in the range of 8 to 9. It has been observed that increase in concentration of bicarbonate fasten rate of settlement and organizes the structure of sample. Based on these evidences, pH could be the main reason for card-house structure of MFT not bicarbonate.

In next chapter, equations of consolidation for both saturated and unsaturated MFT are solved and model predictions are compared to experimental results.

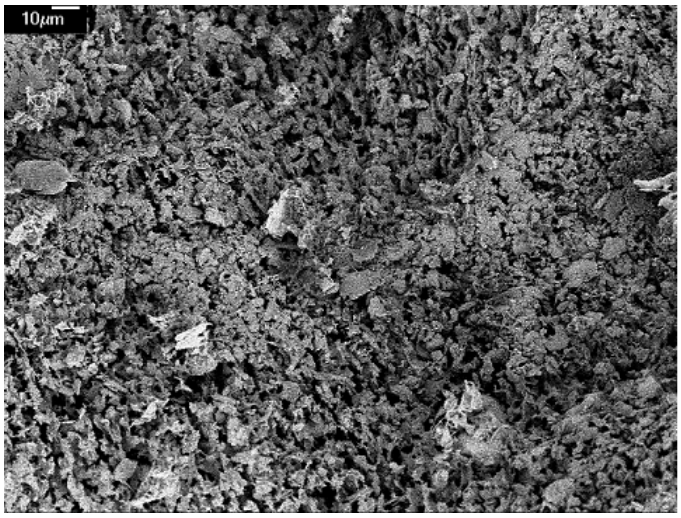

Figure 4.15: Structure of synthetic fines without $NaHCo_3$ (500x)

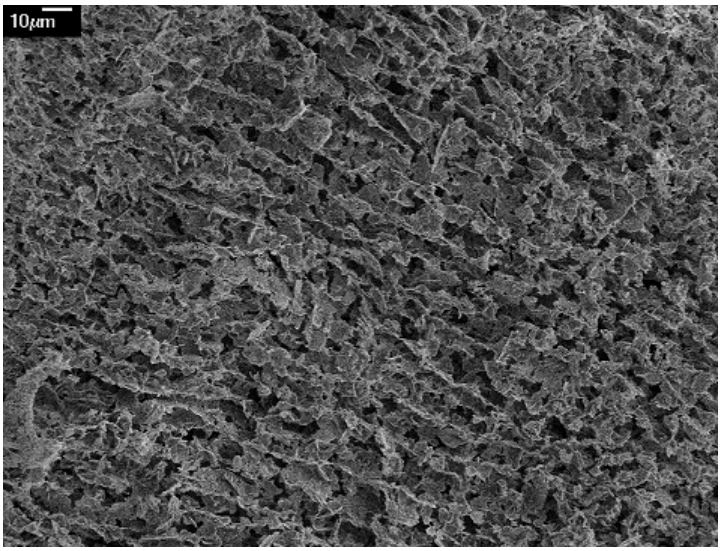

Figure 4.16: Structure of synthetic fines with 2000 ppm $NaHCo_3$(500x)

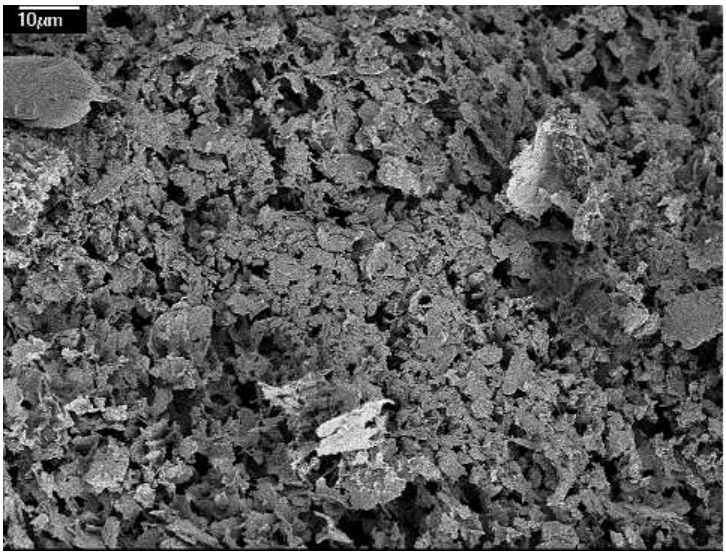

Figure 4.17: Structure of synthetic fines without $NaHCo_3$ (1000x)

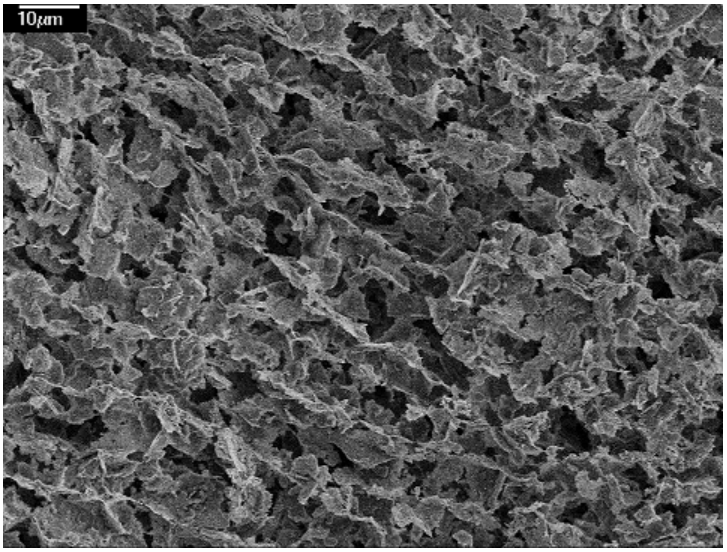

Figure 4.18: Structure of synthetic fines with 2000 ppm $NaHCo_3$(1000x)

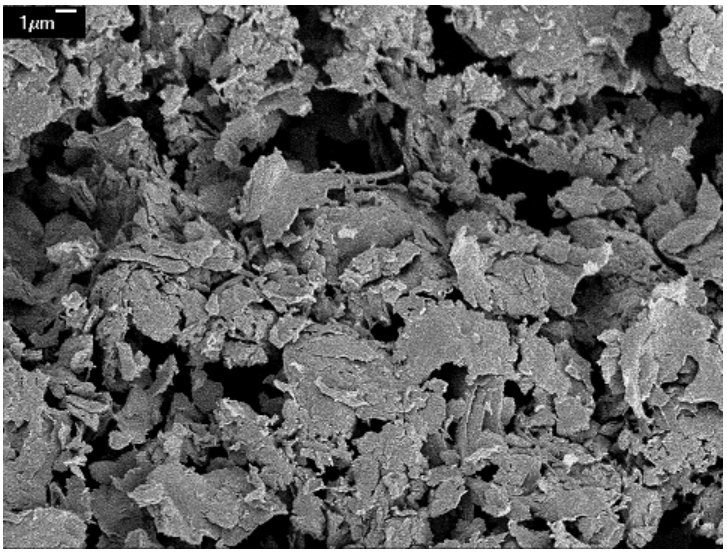

Figure 4.19: Structure of synthetic fines without $NaHCo_3$ (3500x)

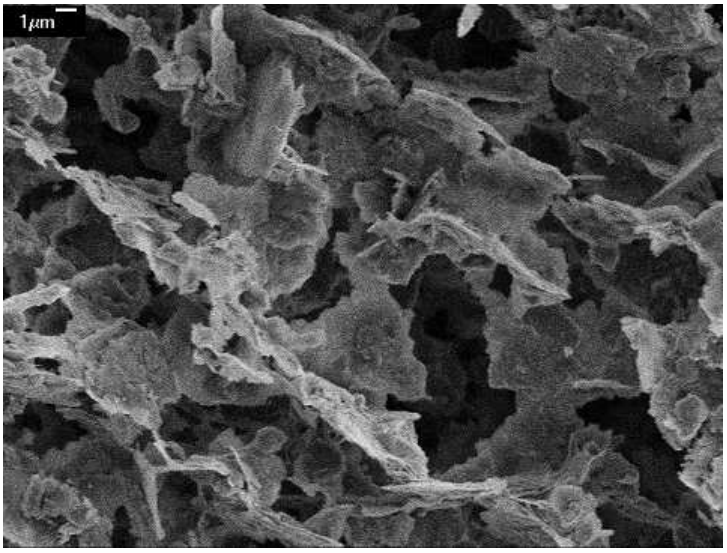

Figure 4.20: Structure of synthetic fines with 2000 ppm $NaHCo_3$(3500x)

Chapter 5

Modeling Results

5.1 Numerical methods

Analysis of a problem means to solve it through equations, but numerical analysis is referred to solve problems by using arithmetic procedures such as; addition, subtraction, multiplication, division. Analytical methods for solving equations are not applicable when; the partial differential equation (PDE) is not linear and cannot be linearized, the boundary conditions are mixed or time-dependent, and the medium is inhomogeneous.

5.1.1 Steps in solving the problems

Gerald and Wheatley (1915) mentioned four general steps which are essential to follow for solving a scientific or an engineering problem.

1. Understand the problem clearly and simplify assumptions.

2. Describe the problem with differential equations that could be solved by numerical methods. Determine boundary and initial conditions

3. Solve the equations, and find numerical answers.

4. Interpret the results of equations.

5.1.2 Finite Difference Method

Finite Difference Method (FDM) is based on approximating the differential operator by replacing the derivatives in the equation using differential quotients. The FDM analysis involves following steps: Generating a grid; Replacing derivatives in equation with finite difference schemes; Assembling the matrix of coefficients; and Solving the algebraic equations. In next section, important schemes of FDM are discussed.

5.1.2.1 Euler's method

This method utilizes the definition of derivative to simplify the equations. Therefore, the term $\frac{du}{dt}$ in the equations defines as

$$\frac{u(t+h)-u(t)}{h} \approx \frac{du}{dt} \tag{5.1}$$

where h is not zero but really small.

Independent parameters should be discretized by

$$x_0 < x_1 < ... < x_{n-1} < x_N \tag{5.2}$$

$$h = step\,size = x_1 - x_0 \tag{5.3}$$

There is a dependent parameter for each independent parameter as

$$y_0, y_1, ..., y_N \tag{5.4}$$

All derivatives and parameters are substituted according to their mesh values. Initial and boundary values are known, therefore values for next points in domain are calculated based on previous points. By this way, all values in domain are calculated.

Euler's method is divided into three categories based on definition of derivatives: forward Euler, backward Euler (or implicit Euler), and trapezoidal.

For instance, derivatives are replaced based on following equation in forward Euler

$$f'(x_0) \approx \frac{f(x_0 + \triangle x) - f(x_0)}{\triangle x} \tag{5.5}$$

and in backward Euler this equation is

$$f'(x_0) \approx \frac{f(x_0) - f(x_0 - \triangle x)}{\triangle x} \tag{5.6}$$

and in central

$$f'(x_0) \approx \frac{f(x_0 + \triangle x) - f(x_0 - \triangle x)}{2\triangle x} \tag{5.7}$$

These equations are calculated based on Taylor's series (Gerald and Wheatley, 1915).

5.2 Solution to finite strain equation

As explained in part 3.3, one-dimensional consolidation equation for saturated soil is

$$\pm\left(\frac{\rho_s}{\rho_f}-1\right)\frac{d}{de}\left[\frac{k\left(e\right)}{1+e}\right]\frac{\partial e}{\partial z}+\frac{\partial}{\partial z}\left[\frac{k\left(e\right)}{\rho_f(1+e)}\frac{\partial\sigma'}{\partial e}\frac{\partial e}{\partial z}\right]+\frac{\partial e}{\partial t}=0 \tag{5.8}$$

which is highly non-linear. In this part, numerical solution for this equation is discussed.

5.2.1 Linearized finite strain equation

To overcome the difficulty of solving a nonlinear equation, Gibson et al. (1989) came up with finite strain coefficient of consolidation. They described this coefficient as

$$g(e)=-\frac{k(e)}{\rho_f}\frac{1}{1+e}\frac{d\sigma'}{de} \tag{5.9}$$

They found out that $g(e)$ is much less sensitive to changes of void ratio than individual parameters in the function. Therefore, they suggested that $g(e)$ can be considered as constant parameter in equation of consolidation. By this assumption, equation 5.8 changes to

$$\frac{\partial^2 e}{\partial z^2}\pm\left(\rho_s-\rho_f\right)\frac{d}{de}\left[\frac{de}{d\sigma'}\right]\frac{\partial e}{\partial z}=\frac{1}{g}\frac{\partial e}{\partial t} \tag{5.10}$$

However, the equation 5.8 is still nonlinear, and needs some more modifications. Gibson et al. (1989) described a new parameter $\lambda(e)$ as

$$\lambda(e)=-\frac{d}{de}\left(\frac{de}{d\sigma'}\right) \tag{5.11}$$

They assumed λ as a constant parameter, and derived the relation between void ratio and effective stress as

$$e = (e_{00} - e_{\infty})exp(-\lambda\sigma') + e_{\infty} \tag{5.12}$$

where e_{00} is void ratio at the beginning of consolidation,

and e_{∞} is void ratio at the end of consolidation.

Through these assumptions, they converted one dimensional consolidation equation of homogeneous soil to

$$\frac{\partial^2 e}{\partial z^2} \pm \lambda\left(\rho_s - \rho_f\right)\frac{\partial e}{\partial z} = \frac{1}{g}\frac{\partial e}{\partial t} \tag{5.13}$$

which is linear , and easy to solve.

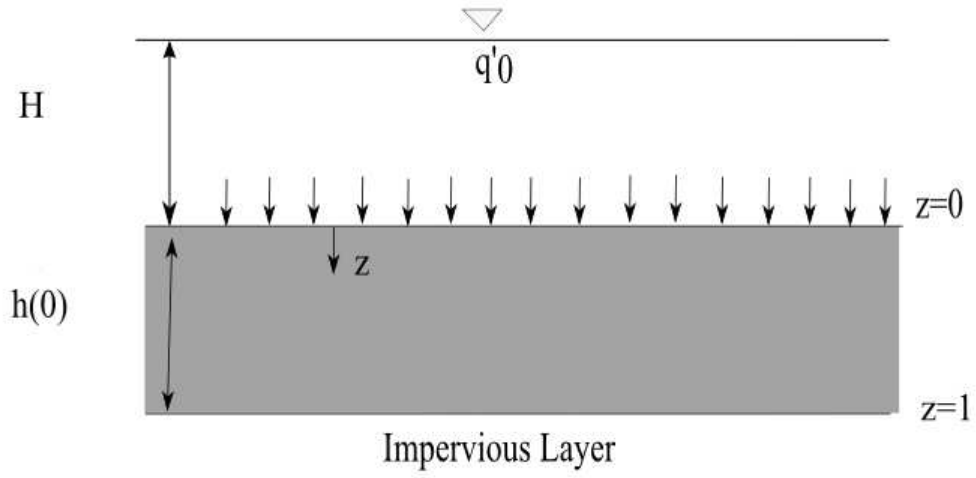

Figure 5.1: Homogeneous clay layer (modified from Gibson et al. (1989))

It is essential to define boundary and initial conditions in order to solve equation 5.13. Consider a layer of saturated soil with impervious bottom and previous upper layer, which consolidates under its own weight and external

stress q'_0 (Figure 5.1). For this soil layer, boundary conditions are;

Initial condition

$$\sigma'(z,0) = q'_0 + (\rho_s - \rho_f)z \tag{5.14}$$

By combination of equations 5.12 and 5.14, void ratio at $t = 0$ is

$$e(z,0) = (e_{00} - e_\infty)exp(-\lambda[q'_0 + (\rho_s - \rho_f)]) + e_\infty \tag{5.15}$$

Upper boundary condition

$$e(0,t) = (e_{00} - e_\infty)exp(-\lambda[q'_0 + \rho_f H]) + e_\infty \tag{5.16}$$

where H is height of released water on top of soil layer.

Lower boundary condition (impervious boundary)

$$v_s = v_f \tag{5.17}$$

and by substituting 5.17 into equation 3.35 and subtracting from 3.24, lower boundary condition is

$$\frac{\partial e}{\partial z} + (\rho_s - \rho_f)\frac{de}{d\sigma'} = 0 \tag{5.18}$$

Gibson et al. (1989) applied explicit finite difference method to solve this equation for thick, loaded, homogeneous clay layers. They compared final results with conventional consolidation theories (Terzaghi's) and concluded that conventional theory overestimates time of consolidation but underestimates excess pore-water pressure at each time. However, they acknowledged that finite strain coefficient of consolidation is not constant during consolidation, and therefore their initial assumption is questionable.

5.2.2 Non-linear finite strain consolidation

The approach by Somogyi is used to solve governing equation of consolidation in this study.

5.2.2.1 The approach by Somogyi

Somogyi (1980) reformed the governing equation of consolidation by Koppula (1970) and presented it in terms of pore-water pressure instead of void ratio;

$$\frac{\partial}{\partial z}\left[-\frac{k}{(1+e)\,\gamma_f}\frac{\partial u}{\partial z}\right]+\frac{de}{d\sigma'}\frac{\partial \sigma'}{\partial t}=0 \tag{5.19}$$

Based on equation 3.31, time dependent equation for effective stress is

$$\frac{\partial \sigma'}{\partial t}=(G-1)\,\gamma_f\frac{d(\triangle z)}{d\sigma'}-\frac{\partial u}{\partial t} \tag{5.20}$$

where G is relative density of solid ($\frac{\rho_s}{\rho_f}$),

and $\triangle z$ is reduce coordinate difference between surface and any point in the system.

By substituting equation 5.20 in equation 5.19, new governing equation is defined by Somogyi (Winnipeg 1980) in term of excess pore-water pressure

$$\frac{\partial}{\partial z}\left[-\frac{k}{(1+e)\,\gamma_f}\frac{\partial u}{\partial z}\right]+\frac{de}{d\sigma'}\left\{(G-1)\,\gamma_f\frac{d(\triangle z)}{d\sigma'}-\frac{\partial u}{\partial t}\right\}=0 \tag{5.21}$$

Also he assumed that there is a power law relationship for effective stress-void ratio and permeability-void ratio

$$e = A\sigma'^{B} \tag{5.22}$$

$$k = Ce^{D} \tag{5.23}$$

where A, B, C and D are constant parameters and determined by consolidation test as explained in part (4.4).

By substituting equations of compressibility and permeability (5.22 and 5.23) in equation 5.21, finite strain equation of consolidation is

$$\frac{\partial u}{\partial t} + \frac{\sigma'^{B}}{\alpha}\left(\frac{k}{1+e}\right)\frac{\partial^2 u}{\partial z^2} + \frac{\sigma'^{B}}{\alpha}\frac{\partial\left(\frac{k}{1+e}\right)}{\partial z}\frac{\partial u}{\partial z} = \gamma_b \frac{d\left(\triangle z\right)}{dt} \tag{5.24}$$

$$\alpha = AB\gamma_w \tag{5.25}$$

$$\beta = 1 - B \tag{5.26}$$

$$\gamma_b = \gamma_s - \gamma_f \tag{5.27}$$

where γ is specific gravity.

Implicit finite difference method is used to ensure stability of solution for equation 5.24. Term $(\frac{d(\triangle z)}{dt})$ defines accumulation in the system. There is not any insert flow for the system in this study, this term is negligible.

After breaking down the derivatives to the finite difference terms and substi-

tuting required parameters, finite strain equation converts to

$$\frac{u\,(i,j+1)-u\,(i,j)}{\triangle t}+\frac{\sigma(i,j)'^{B}}{\alpha}\left\{\frac{u\,(i+1,j+1)-2u\,(i,j+1)-u(i-1,j+1)}{\triangle z^{2}}\right\}$$
$$(\frac{k(i,j)}{1+e(i,j)})+\frac{\sigma(i,j)'^{B}}{\alpha}\frac{1}{4\triangle z^{2}}\left(\frac{k(i+1,j)}{1+e(i+1,j)}-\frac{k(i-1,j)}{1+e(i-1,j)}\right)$$
$$[u(i+1,j+1)-u(i-1,j+1)]=\gamma_{b}\frac{d\,(\triangle z)}{dt} \tag{5.28}$$

Following parameters are defined in equation 5.28 to reduce number of parameters and avoid confusion

$$(u(i,j+1)-u(i,j))+E_{ij}K_{ij}\delta\,(u\,(i+1,j+1))-2E_{ij}\delta K_{ij}u(i,j+1)$$
$$+u(i-1,j+1))+E_{ij}L_{ij}\delta(u(i+1,j+1)-u(i-1,j+1))=0 \tag{5.29}$$

where

$$E_{ij}=\frac{\sigma'_{ij}}{\alpha} \tag{5.30}$$

$$K_{ij}=\frac{k_{ij}}{1+e_{ij}} \tag{5.31}$$

$$L_{ij}=\frac{1}{4}\left(\frac{k(i+1,j)}{1+e(i+1,j)}-\frac{k(i-1,j)}{1+e(i-1,j)}\right) \tag{5.32}$$

$$\delta=\frac{\triangle t}{\triangle z^{2}} \tag{5.33}$$

By rearranging equation 5.29, pore-water pressure at point i and at time j is defined as

$$u(i,j)=E_{ij}\delta\,(K_{ij}+L_{ij})\,u(i+1,j+1)+(1-2E_{ij}\delta K_{ij})(u(i,j+1))$$
$$+E_{ij}\delta\,(K_{ij}-L_{ij})\,u\,(i-1,j+1)$$

Boundary conditions

Lower boundary Lower boundary is impervious

$$\frac{\partial u}{\partial z}|_{z=0} = 0 \tag{5.34}$$

It is converted to finite difference form

$$u_{i+1} - u_{i-1} = 0 \tag{5.35}$$

and in by substituting it in the main equation, it results;

$$2E_{ij}\delta K_{ij}u_{i+1,j} + (1 - 2E_{ij}\delta K_{ij})u_{i,j+1} = u_{i,j} \tag{5.36}$$

Upper Boundary Excess pore-water pressure is assumed zero in upper boundary due to its connection to released water

$$u_{i+1,j+1} = 0 \tag{5.37}$$

Initial Condition Initial void ratio is calculated according to known initial solid content, S_{in}, by following equation

$$e_0 = G\left(\frac{1 - S_{in}}{S_{in}}\right) \tag{5.38}$$

Based on initial void ratio and equations of compressibility and permeability, initial effective stress and permeability are

$$\sigma'_0 = \left(\frac{e_0}{A}\right)^{\frac{1}{B}} \tag{5.39}$$

$$k_0 = Ce_0^D \tag{5.40}$$

The final equation is according to the Reduced coordinate z, which relates height of sample to volume of solid. To convert the height of sample to Reduced coordinate, following equation is used.

$$z = \frac{H}{1 + e_0} \tag{5.41}$$

To solve the equations, matrix of coefficients and constants are assembled (i changes from 1 to $n-1$, and j from 0 to N). Excess pore-water pressures are calculated;

$$\begin{bmatrix} 1 - 2E_1\delta K_1 & 2E_1\delta K_1 & ... & 0 \\ E_2\delta\left(K_2 - L_2\right) & 1 - 2E_2\delta K_2 & E_2\delta\left(K_2 - L_2\right) & ... \\ ... & ... & ... & ... \\ 0 & ... & E_{n-1}\delta\left(K_{n-1} - L_{n-1}\right) & 1 - 2E_{n-1}\delta K_{n-1} \end{bmatrix} \begin{bmatrix} u_{1,j+1} \\ u_{2,j+1} \\ ... \\ u_{n-1,j+1} \end{bmatrix} = \begin{bmatrix} u_{1,j} \\ u_{2,j} \\ ... \\ u_{n-1,j} \end{bmatrix} \tag{5.42}$$

A MATLAB program has been developed to solve the set of equations in equation 5.42. Effective stresses in different locations and time are calculated by use of calculated excess pore-water pressure and the following equation;

$$\sigma'(z) = \sigma'_0 + \sigma_b(z) - u(z) \tag{5.43}$$

$$\sigma_b(z) = \gamma_b(\triangle z) \tag{5.44}$$

where $\gamma_b = \gamma_w(G-1)$,

Effective stress in terms of height h is

$$\sigma_b(z) = \frac{\gamma_s - \gamma_w}{1+e}(h_{top} - h) \tag{5.45}$$

New void ratio is calculated according to equations of compressibility (effective stress-void ratio) and permeability (hydraulic conductivity-void ratio) and calculated effective stress. Height of slurry is obtained according to new void ratio and the following equation;

$$h = \int_0^H (1+e)dz \tag{5.46}$$

Also, a model is developed in COMSOL Multiphysics to solve governing equation of consolidation, which is described in the next section.

5.2.3 COMSOL theoretical background

COMSOL Multiphysics is a commercial software to solve partial differential equations based on finite element methods. The finite element method is a numerical technique in which solution is approximated by a shape function

in each grid. In this method, the equation is multiplied by a shape function and integrated over the domain. Transformed equation is called weak form which is basis of solver in COMSOL. The mathematical weak form gives complete flexibility in defining finite element problems. In this section, theoretical background for deriving the weak form in this software is described briefly.

Deriving the weak form Consider the following equation which is a two dimensional (2D) PDE for a single dependent variable, u.

$$\nabla.\Gamma = F \quad in\ \Omega \tag{5.47}$$

$$\Gamma = g_D \ \ on\ \partial\Omega_D \quad \nabla\Gamma.n = g_N \ \ on\ \partial\Omega_N \tag{5.48}$$

In order to find a unique solution for the equation 5.47, boundary conditions are needed in some parts of the domain Ω. Drichlet boundary conditions specified the value of Γ along some region of boundary denoted by $\partial\Omega_D$. A Neumann boundary specifies the value of $\nabla\Gamma$ along some boundary that is called $\partial\Omega_N$. These segments do not overlap and their combination gives us the whole domain $\partial\Omega$. Assume ν as an arbitrary function on the same domain Ω, which is called test function. If we multiply the equation 5.47 to test function (ν) and integrate, the equation will change to

$$\int_\Omega \nu\nabla.\Gamma dA = \int_\Omega \nu F dA \tag{5.49}$$

where dA is element of area.

After using Green's formula, equation 5.49 converts to

$$\int_{\partial\Omega} \nu\Gamma.ndA - \int_{\Omega} \nabla.\nu\Gamma dA = \int_{\Omega} \nu F dA \tag{5.50}$$

where ds is length element. By considering Neumann boundary condition

$$-n.\Gamma = G + \frac{\partial R}{\partial u}\mu \tag{5.51}$$

equation 5.50 changes to

$$\int_{\Omega} (\nabla\nu.\Gamma + \nu F)dA + \int_{\partial\Omega} \nu(G + \frac{\partial R}{\partial u}\mu)ds = 0 \tag{5.52}$$

Equation 5.52 with Drichlet condition is the weak reformation of the PDE problem.

Partial differential equation in COMSOL Multiphysics is defined as equation 5.53, and it can be used to model variety of problems. The parameters in the equation are defined in the Table 5.1.

$$e_a\frac{\partial^2 u}{\partial t^2} + d_a\frac{\partial u}{\partial t} - \nabla.(c\nabla u + \alpha u - \gamma) + \beta.\nabla u + au = f \tag{5.53}$$

where $e_a\frac{\partial^2 u}{\partial t^2}$ is mass term,

$d_a\frac{\partial u}{\partial t}$ is damping/mass term,

$(c\nabla u + \alpha u - \gamma)$ is conservative flux term,

and $\beta.\nabla u$ is convection term.

Parameters	definition
e_a	mass coefficient
d_a	damping coefficient or mass coefficient
c	diffusion coefficient
α	conservative flux convection coefficient
β	convection coefficient
a	absorption coefficient
γ	conservative flux source term
f	source term

Table 5.1: Definition of parameters in partial differential equation in COMSOL

5.3 Modeling results

5.3.1 Saturated MFT

One-dimensional finite strain consolidation equation is used to simulate settlement of particles in saturated MFT. COMSOL Multiphysics is used to solve the equations of consolidation based on Somogyi's approach. Different parameters in equation 5.53 are defined to present equation of consolidation (equation 5.21).

5.3.1.1 Model prediction for 10 m standpipe experiment

To investigate consolidation behaviour of oil sands tailings, three standpipes were installed in 1982 at University of Alberta. Different experiments have been conducted to understand settling characteristics of these MFT samples since 1982.

Experimental results including rate of consolidation and compressibility and permeability parameters are used to verify results of developed model. These experimental data are reported by (Jeeravipoolvarn, 2005; Suthaker, 1995; Pollock, 1988).

Parameters	A ($\frac{1}{Pa}$)	B	C ($\frac{m}{s}$)	D
	28.71	-0.3097	7.425e-11	3.847

Table 5.2: Compressibility and permeability parameters for standpipe 1

Initial solid content	32.4 wt%
Specific gravity of solid (G_s)	2.84
Bulk density ($\frac{kg}{m^3}$)	1221
Initial height of tailings (m)	10

Table 5.3: Constant and initial parameters for standpipe 1

Based on parameters in Tables (5.2 and 5.3), finite strain theory is solved and results are shown in Figure 5.4 along with experimental observations from standpipe 1 for about 4.5 years . There is a qualitative agreement between model prediction and experimental observations. Model predicts long term results (shown in Figure 5.3) with more accuracy as consolidation is a slow process and it takes decades for this process to be completed. Also, modeling results are very sensitive to coefficient of compressibility and permeability. Deviation of model from experimental results may arise from error in measuring coefficient of permeability and compressibility.

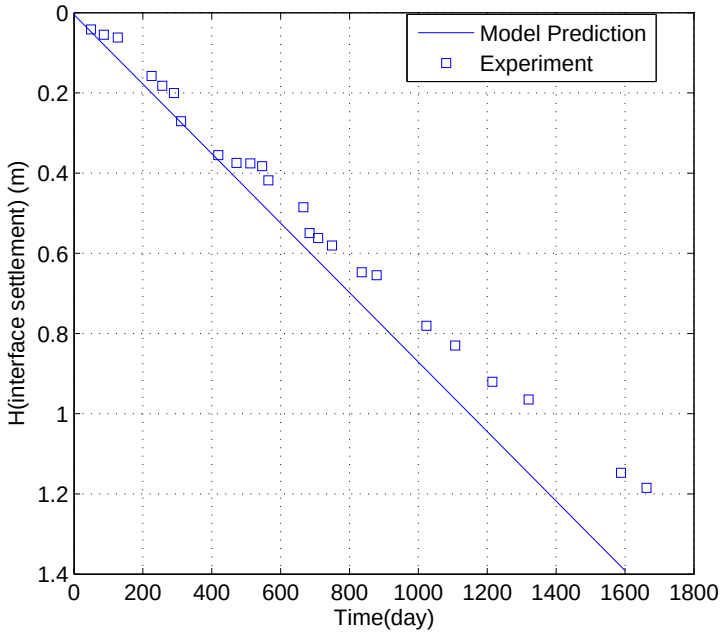

Figure 5.2: Settlement of MFT (comparison of model prediction with experimental results)

5.3.1.2 Model prediction for long term consolidation process

Simulation results by Jeeravipoolvarn (2005) for $10\,m$ standpipe are used to verify developed model in this study. Parameters are substituted according to Tables (5.4 and 5.5).

Parameters	A ($\frac{1}{KPa}$)	B	C ($\frac{m}{day}$)	D
	7.72	-0.22	2.532e-7	4.65

Table 5.4: Compressibility and permeability parameters

Initial solid content	16 wt%
Specific gravity of solid (G_s)	2.82
Initial height of tailings (m)	9.6

Table 5.5: Constant and initial parameters

Results of this simulation are in well agreement with Jeeravipoolvarn results as shown in Figure 5.3. The slight difference may arise from differences in numerical methods which were used to solve the equation.

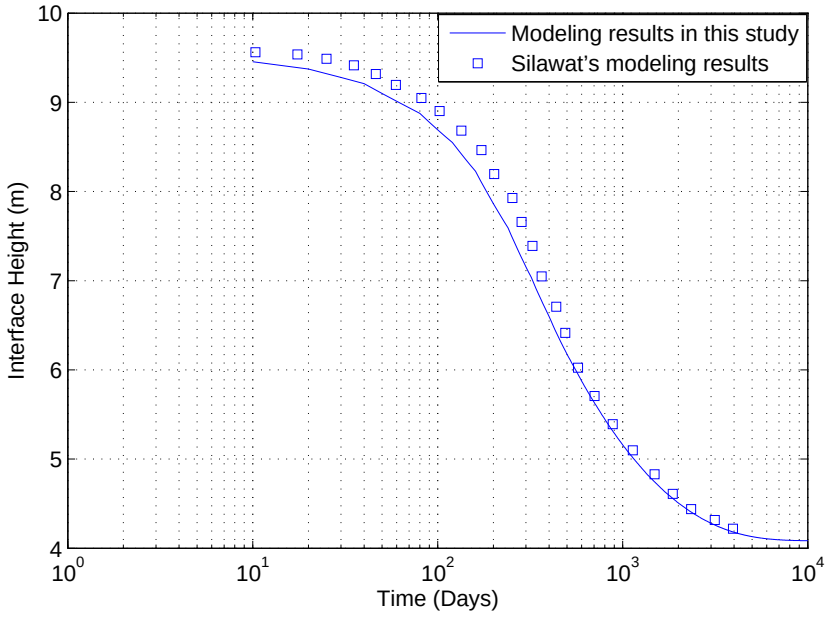

Figure 5.3: Comparison of solid settlement (this study and Jeeravipoolvarn (2005))

5.3.1.3 Model prediction for $2\,m$ standpipe (saturated)

As described in part (4.1), $2\,m$ standpipes are installed to investigate effects of microbial activity in settlement of MFT. Coefficient of compressibility and permeability ($e = A\sigma'^{B}$, $k = Ce^{D}$) for unamended MFT in $2\,m$ column are predicted in this section, which are essential for predicting rate of settlement.

Initial parameters are based on Pollock (1988) and Suthaker (1995)'s studies on MFT (Tables 5.6 and 5.7).

Parameters	A ($\frac{1}{Pa}$)	B	C ($\frac{m}{s}$)	D
	28.71	-0.3097	7.425e-11	3.847

Table 5.6: Initial consolidation parameters by Pollock (1988)

Parameters	A ($\frac{1}{Pa}$)	B	C ($\frac{m}{s}$)	D
	54.11	-0.3224	6.16e-11	4.468

Table 5.7: Initial consolidation parameters by Suthaker (1995)

These Coefficients of consolidation have been optimized to match the experimental results. Optimized parameters are given in Table 5.8. The results of experiment and model prediction with parameters in Tables (5.6 and 5.7) are illustrated in Figures (5.4 and 5.5).

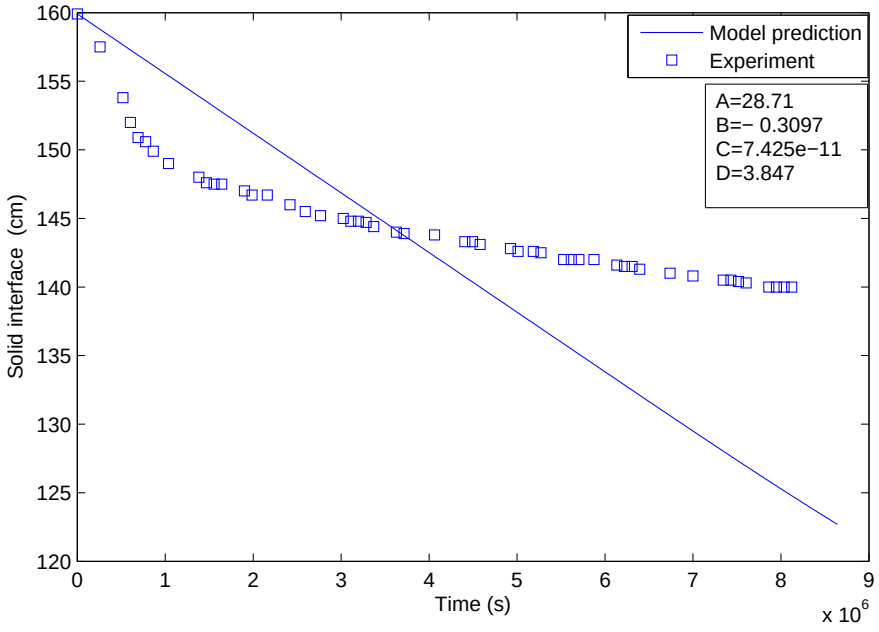

Figure 5.4: Model prediction for experimental observation from 2 m columns (according to compressibility and permeability parameters by Pollock (1988))

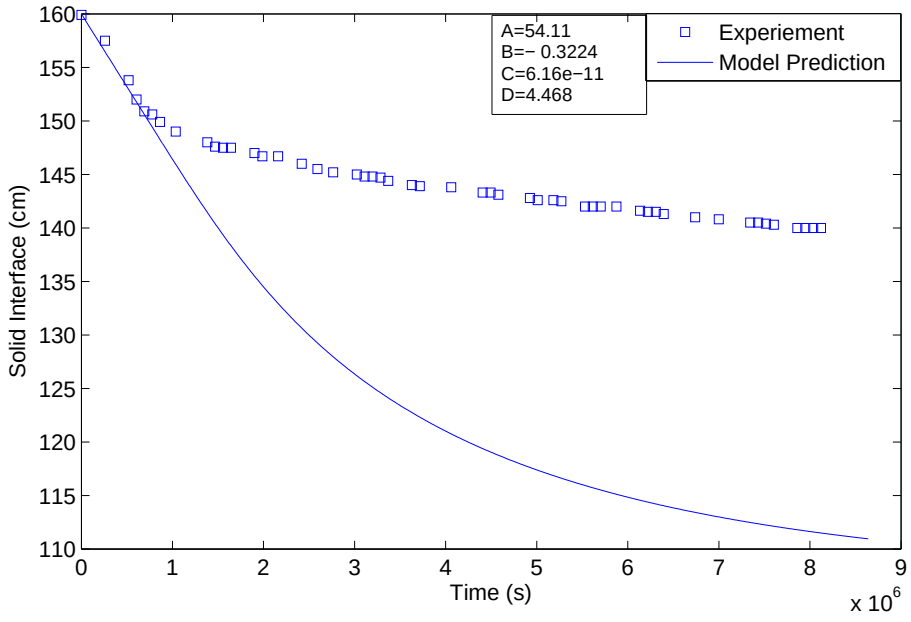

Figure 5.5: Model prediction for experimental observation from 2 m columns (according to compressibility and permeability parameters by Suthaker (1995))

There is a substantial difference between model prediction and experimental observations with consolidation parameters in Tables (5.6 and 5.7). These differences arise from difference in initial solid concentration, origin and structure of MFT samples. In order to reduce the error, compressibility and permeability parameters are changed and the best fits are shown in Figure 5.7 and Table 5.8.

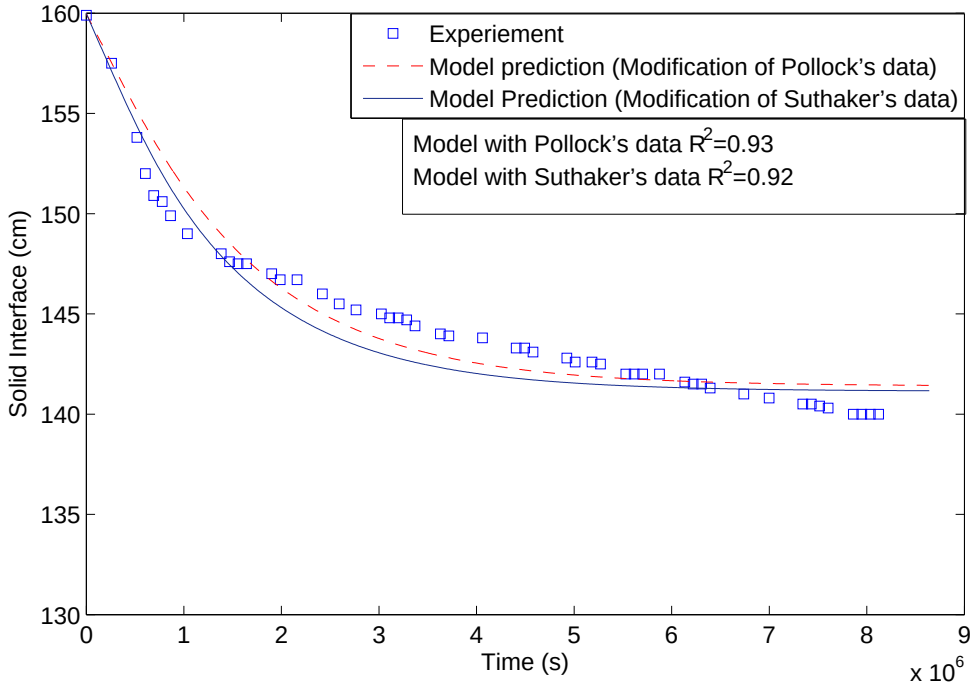

Figure 5.6: Model prediction with experimental observation for unamended MFT $2\,m$ column (modified compressibility and permeability parameters)

	Compressibility		Permeability	
Constant parameters	A $(\frac{1}{Pa})$	B	C $(\frac{m}{s})$	D
Modification for Pollock's parameters	69	-0.28	16e-11	3.847
Modification for Suthaker's parameters	100	-0.3224	5e-11	4.468

Table 5.8: Modified compressibility and permeability parameters

5.3.2 Effects of ion concentration on hydraulic conductivity

Effect of chemical ions in settlement of particles is investigated by installing $2\,L$ columns with different bicarbonate ion concentration as discussed in part (4.6). Based on the experimental observations of $2\,L$ columns, it is proposed that bicarbonate anions increase rate of settlement by forming an organized structure. It is assumed that organized structure improves permeability of water through soil and results in faster settlement.

In order to study effect of bicarbonate ions in permeability of soil, coefficients of permeability and compressibility are predicted by matching results of experiment with model. Experimental results and model prediction are compared in Figures (5.7, 5.8, and 5.9).

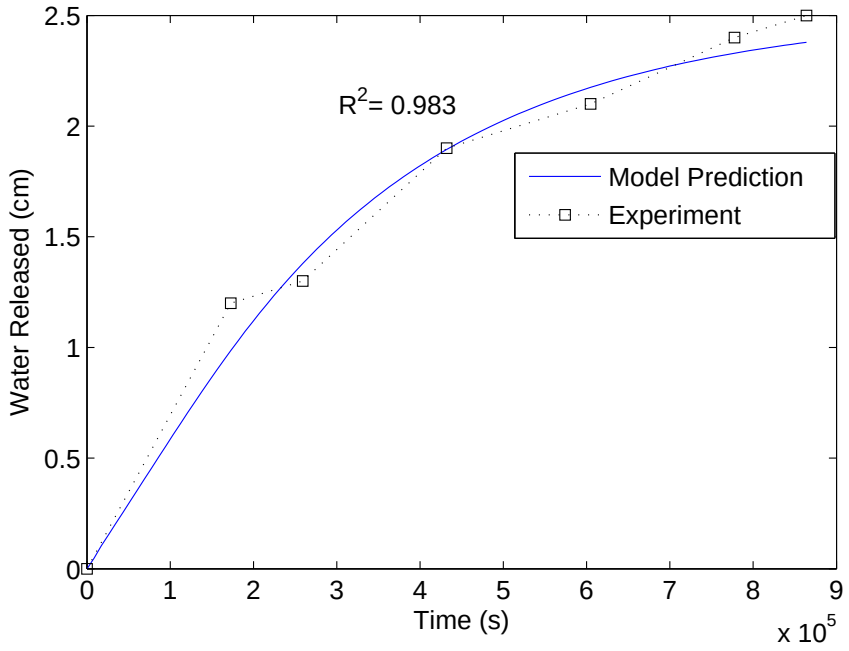

Figure 5.7: Model prediction for settlement of solids in $2\,L$ column ($2000\,ppm$)

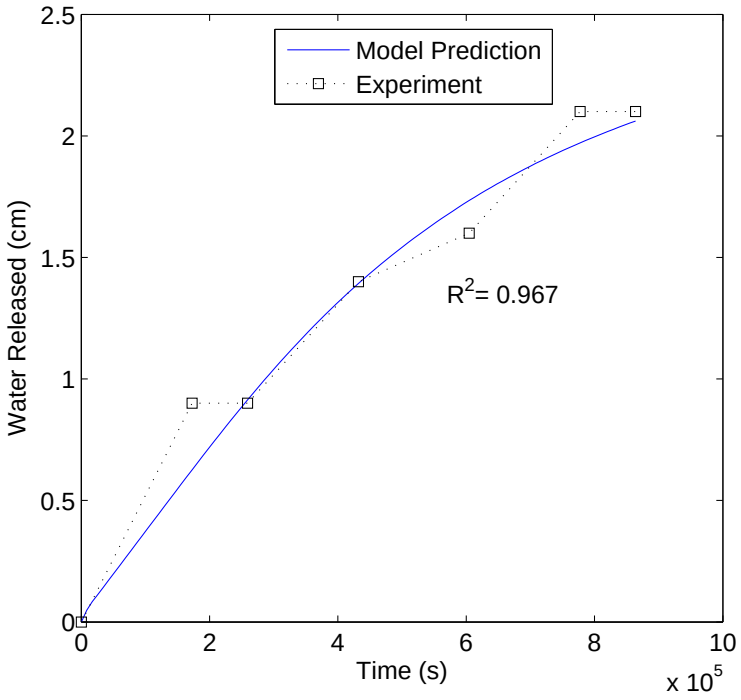

Figure 5.8: Model prediction for settlement of solids in 2 L column (1000 ppm)

Hydraulic conductivity is calculated based on predicted coefficient of permeability for slurry with different concentration of bicarbonate ions. As illustrated in Figure 5.10, bicarbonates cause increase in hydraulic conductivity of slurry. This increase could be one of the main reasons for faster settlement of particles with higher concentration of bicarbonates.

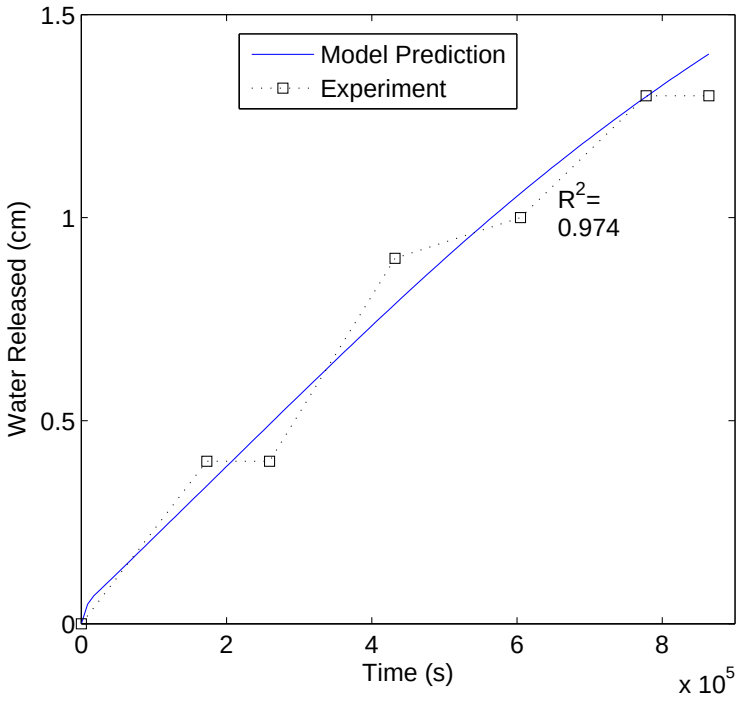

Figure 5.9: Model prediction for settlement of solids in 2 L column (500 ppm)

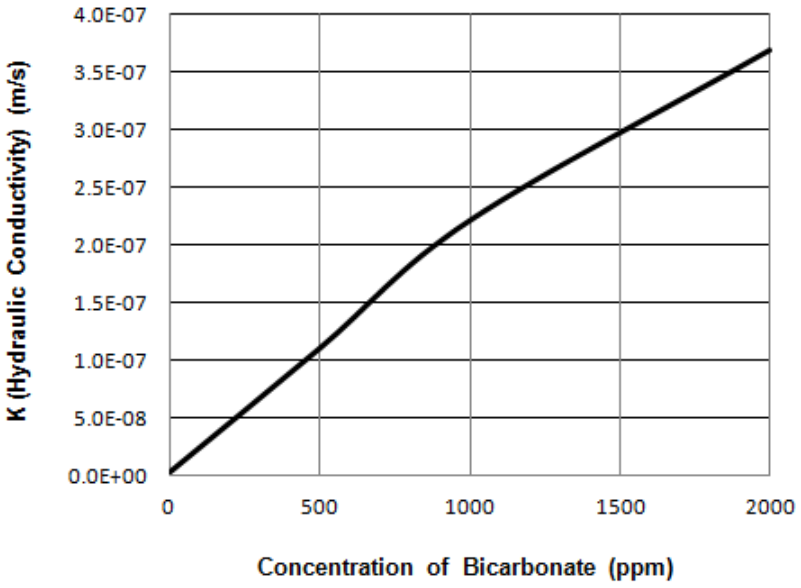

Figure 5.10: Effect of bicarbonate ions on permeability of soil

5.3.3 Unsaturated MFT

There are gas bubbles stagnant and moving in bio-activated tailing. Effect of stagnant gas bubbles on settling characteristic of MFT is investigated in this study. As discussed before, finite strain equation of consolidation for unsaturated soil (gassy soil) is modified as

$$\frac{\partial e_f}{\partial t} = -\frac{\partial e_f}{\partial z}\frac{\partial}{\partial e_f}\left[\frac{k(e_f)}{\gamma_f(1+e_f+e_g)}\left\{(\gamma_s-\gamma_f(1+e_g))+\frac{\partial \sigma_{op}(e_f)}{\partial z}\right\}\right] + \frac{\frac{\partial e_g}{\partial z}}{(1+e_f+e_g)^2}\frac{k(e_f)}{\gamma_f}\left[(\gamma_s+\gamma_f e_f)+\frac{\partial \sigma_{op}(e_f)}{\partial z}\right] \quad (5.54)$$

Finite strain consolidation for gassy soil (equation 5.54) is solved based on experimental observations by Wichman (1999) (BIO7 test). This test was performed on Slufter mud at room temperature. Similar to bio-activated MFT, gas was produced gradually in Slufter mud by bacteria. After 70 days, total gas content of slurry reported as 8 %. Therefore, experimental observations on this mud are selected to verify model. Total gas content is assumed constant, 8 % in this study.

Consolidation parameters (compressibility and permeability) for this mud are measured by consolidation test and described in following forms;

$$\sigma_{op}(e_f) = \sigma_0 exp(m_1 + m_2 e_f) \quad (5.55)$$

$$k(e_f) = k_0 exp(m_3 + m_4 e_f) \quad (5.56)$$

where $\sigma_0 = 1\ kPa$, and $k_0 = 1\ \frac{m}{s}$.

Wichman introduced optimum constant parameters as values in Table 5.9 for his numerical solution, however he mentioned that at least three sets of consolidation parameters could be used to describe the oedometer results.

In this study, parameters are modified based on these set of data (Table 5.9). Model prediction along with experimental observations are illustrated in Figure 5.11.

	m_1	m_2	m_3	m_4
BIO7	5.78	-1.19	-26.25	1.47
Modified Parameters	5.78	-1.69	-23.25	1.87

Table 5.9: Constant parameters for compressibility and permeability equations

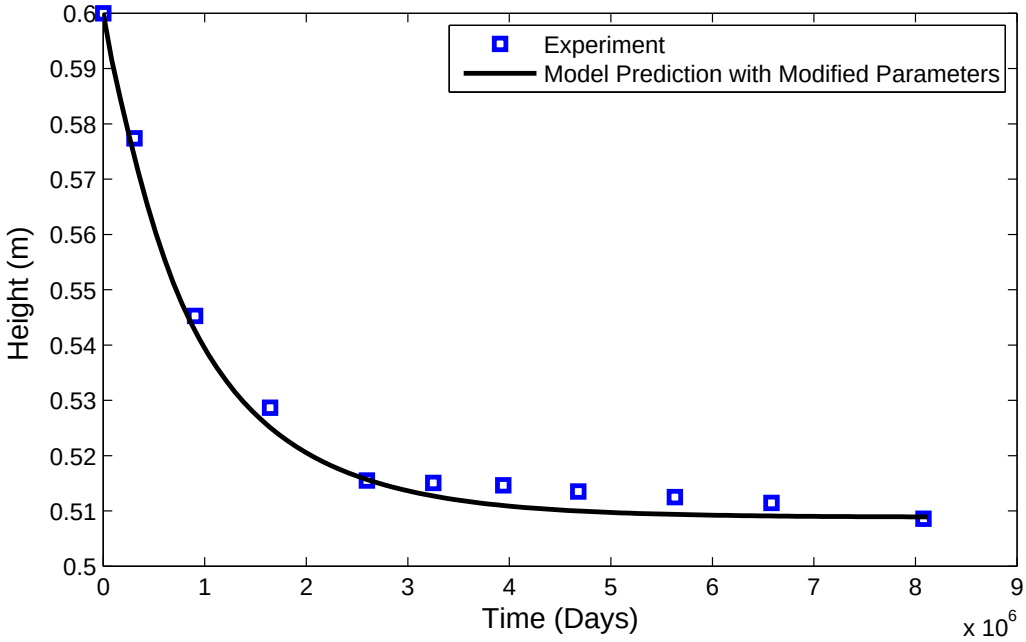

Figure 5.11: Model prediction for gassy slurry (BIO7) with modified parameters

This model predicts consolidation rate of gassy MFT based on finite strain theory. It should be mentioned that there are both stagnant and moving gas bubbles in bio-activated tailings. In this study, stagnant gas bubbles are simulated in MFT. As discussed before, stagnant gas bubbles decrease rate of consolidation in MFT due to density reduction and increase in water drainage path. As illustrated in Figure 5.12 , increasing gas content would reduce the rate of consolidation.

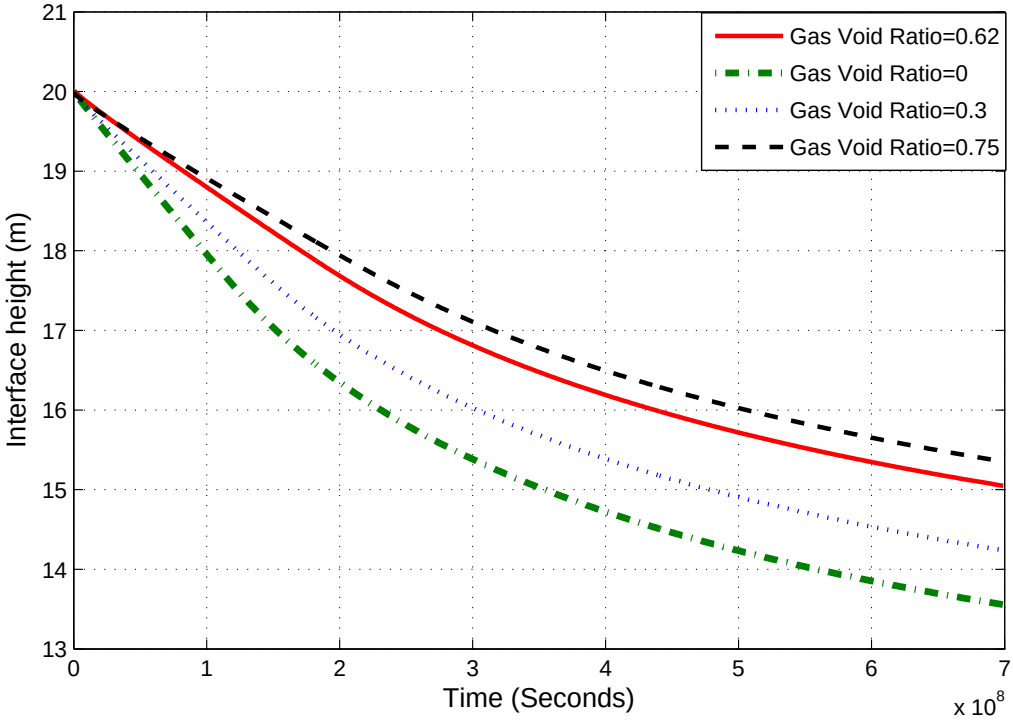

Figure 5.12: Model prediction for settlement of unsaturated soil with different gas content

5.3.3.1 Model prediction for $2\,m$ standpipe (unsaturated)

In this part, settling rate of amended (unsaturated) MFT in $2\,m$ standpipe are predicted by developed model. As discussed earlier, solid interface rose gradually in amended tailings for 48 days and then dropped dramatically. Based on this increment in volume of unsaturated MFT, total gas content is predicted as $8.5\,\%$. Gas content along with compressibility and permeability parameters in Table 5.9, which are measured for case BIO7 by Wichman (1999), are used to predict settling rate of unsaturated soil in standpipe.

Predicted results by developed model matches experimental observations fairly well as illustrated in Figure 5.13. Model does not have the ability to predict rise in solid interface, however it predicts solid interface after collapse quite well.

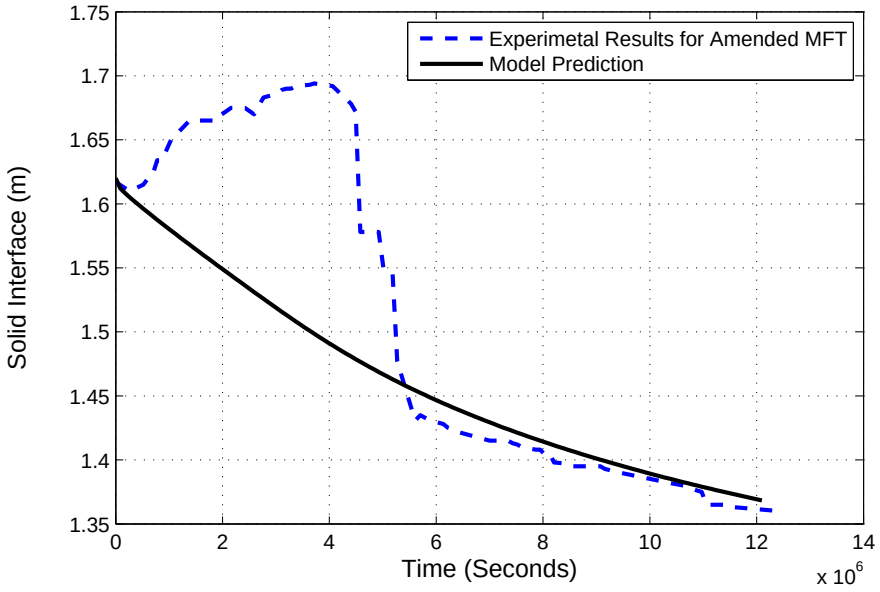

Figure 5.13: Model prediction with experimental observation for amended MFT $2\,m$ column

Chapter 6

Conclusions and Recommendations

Settling process of bio-activated mature fine tailings has been investigated in this study. Two-meter standpipes were installed, one with original MFT and the other with bio-activated (amended) MFT, to study effective factors in process of bio-densification. In amended standpipe, height of sample gradually rose in first 55 days of process due to accumulation of trapped gas in system, and dropped dramatically after collapse in the system. After this collapse, large volume of water in amended MFT released and rate of gas production decreased. Two hypotheses were proposed to describe sudden increase in volume of released water right after collapse of system. First, gas cracks produced by connection of gas bubbles create drainage path for water, and increase consolidation rate in gassy MFT. Also, diameter of gas bubbles increases due to pressure difference between inside and outside of bubbles that compress surrounded soil skeleton and accelerate rate of water release. In unamended case, however there was not any gas production and it was densified gradually.

A model has been developed to describe process of consolidation in saturated MFT (unamended) based on one-dimensional finite strain theory of consolidation.

Developed model was solved based on finite-difference code in MATLAB and then by COMSOL Multiphysics, a commercial solver based on finite-element method. Models were verified with available experimental data in literature and then were used to describe the process in two-meter standpipe. Also, coefficient of compressibility and permeability were estimated tailings in these standpipes. Developed model helps better understanding of influential parameters such as hydraulic conductivity and effective stress in consolidation rate of tailings.

According to chemical analysis and observations, gas production and changes in chemical ions were studied as two main factors in altering settling characteristics of bio-activated tailings. Effects of these parameters were investigated in this study as following.

Effect of gas bubbles There are two types of gas bubbles in amended tailings; first type is trapped gas bubble which causes crack formation in tailings. The other type is moving gas bubble which leaves the sample and was collected in cap. Each type has their own effect on settling characteristic of tailings. To investigate effects of stagnant gas bubbles in the system, a model was developed based on modification of finite strain theory. Based on this model, settling rates of amended MFT in two-meter standpipe were estimated and results were compared with experimental data. According to the model and experimental observations by Thomas (1987), rate of consolidation decreases with increase in content of stagnant bubbles in the system.

Effect of ion concentration MFT is a complex mixture of water, solid and organic matters, which makes it difficult to investigate effects of individual parameters in its settling rate. Therefore, synthesized MFT was prepared in laboratory to investigate effect of ion concentration in rate of consolidation. Solid part of sample was prepared from MFT according to procedure in part (4.3) and had the same particle distribution as original MFT. Slurries with $25\,wt\%$ solid content and bicarbonate ion concentration of $0\,ppm$, $500\,ppm$, $1000\,ppm$, and $2000\,ppm$ were prepared and placed in graduated cylinders. Settling results showed increase in rate of settlement by increase in concentration of bicarbonate anion. Results from SEM test indicate that bicarbonate ions organize the structure of particles in slurry. As structure of slurry can change its water permeability, hydraulic conductivity test was conducted on samples. Two consolidometers were designed and installed to measure coefficients of compressibility and permeability of slurry. Initial results of hydraulic conductivity test and model prediction for permeability showed an increase in permeability with increase in concentration of bicarbonate ions. Therefore, effect of chemical parameters was proposed as an important factor in increased volume of released water in bio-activated MFT compare to unamended MFT.

Recommendations In this study, effect of gas movement and channeling in settling behaviour of tailings has not been investigated. Further understanding of gas movement and its effect in consolidation is recommended. Also, it is assumed that gas content is well distributed in system and its variation along the height has been neglected. This assumption should be alleviated for further development of model. Bitumen and organic-free MFT could be further used to study of effect of other parameters in consolidation behaviour of MFT.

These parameters include pH, surface chemistry, and particle flocculation. As biological activity in tailings changes ion concentration and surface chemistry of tailings, study of those parameters could be implemented in model to explain increase in volume of released water for amended MFT.

Bibliography

Aiban, S., Znidarcic, D., 1989. Evaluation of the flow pump and constant head techniques for permeability measurements. Geotechnique 39, 655–666.

ASTM, 2004. Standard test methods for one-dimensional consolidation properties of soils using incremental loading. ASTM Standard D18.
URL `www.astm.org`

Auzerais, F., Jackson, R., Russel, W., 1988. The resolurtion of shocks and the effects of compressible sedimentsin transient settling. Fluid Mech. 195, 437–482.

Been, K., 1980. Stress strain behaviour of a cohesive soil deposited under water. Ph.D. thesis, Balliol College, Oxford.

Bishop, A. W., 1959. The principle of effective stress. (text of lecture to the Norwegian Geotechnical Society). Tek. Ukeblad 39, 859–863.

Buscall, R., Goodwin, J., Ottewill, R., Tadros, T., 1982. The settling of particles through Newtonian and non-Newtonian media. Journal of Colloid And Interface Science 85 (1), 78–86.

Chalaturnyk, R. J., Don Scott, J., Ozum, B., 2002. Management of oil sands tailings. Petroleum Science and Technology 20, 1025–1046.

Cooper, P., Harrington, D., 1988. Biotechnology for Engineers. John Wiley & Sons.

Dai, Q., Smith, R., n.d. Electrokinetic study and fine tails treatment. Tech. rep., Syncrude.

Daniel, D., 1989. A note on falling headwater and rising tail water permeability tests. Geotechnical Testing Journal 12, 308–310.

Eckert, W., Masliyah, J., Gray, M., Fedorak, P., 1996. Prediction of sedimentation and consolidation of fine tails. AIChE Journal 42, 960–972.

ERCB, 2009. Tailings Performance Criteria and Requirements for Oil Sands Mining Schemes. Energy Resources Conservation Board.
URL `http://www.ercb.ca`

ERCB, 2011.
URL `http://www.ercb.ca`

Fedorak, P., Coy, D., Dudas, M., Renneberg, A.J., S. M., 2000. Role of microbiological processes on sulfate-enriched tailings deposits. Research Report, Department of Biological Sciences and Department of Renewable Resources, University of Alberta, Edmonton, Alberta.

Fedorak, P., Coy, D., Salloum, M. J., Dudas, M. J., 2002. Methanogenic potential of tailings samples from oil sands extraction plants. Canadian Journal of Microbiology 48, 21–33.

Fedorak, P. M., Coy, D. L., Dudas, M. J., Simpson, M. J., Renneberg, A. J., MacKinnon, M. D., 2003. Microbially-mediated fugitive gas production from oil sands tailings and increased tailings densification rates. Journal of Environmental Engineering & Science 2, 199–211.

FTFC, 1995. Advances in Oil Sands Tailings Research. Alberta Department of Energy, Oil sands and Research Division.

Gerald, C., Wheatley, P. O., 1915. Applied Numerical Analysis. Publisher, Greg Tobin.

Gibson, R., England, G., Hussey, M., 1967. The theory of one-dimensional consolidation of saturated clays. Geotechnique 17, 261–273.

Gibson, R. E., Shiffman, R. L., Whitman, R., 1989. On two definitions of excess pore water pressure. Geotechnique 39, 280–293.

Guo, C., 2009. Rapid densification of the oil sands mature fine tailings (MFT) by microbial activity. Ph.D. thesis, University of Alberta.

Gustafsson, J., Nordenswan, E., Rosenholm, J. B., 2001. Effect of pH on the sedimentation, Zeta-potential, and rheology of anatase suspensions. Colloids and Surfaces A: Physicochemical and Engineering Aspects 212, 235–247.

Hall, E., Tollefson, E., 1982. Stabilization and destabilization of mineral fines-bitumen-water dispersions in tailings from oil sand extraction plants that use the hot water process. Canadian Journal of Chemical Engineering 60, 812–821.

Hill, R., 1965. A self-consistent mechanics of composite materials. Journal of the Mechanics and Physics of Solids 13, 213–222.

Holowenko, F., MacKinnon, M., Fedorak, P., 2000. Methanogens and sulfate-reducing bacteria in oil sands fine tailings wastes. Canadian Journal of Microbial 46, 927–937.

Imai, G., 1981. Experimental studies on sediment mechanism and sediment formation of clay materials. Soils and Foundations 21, 7–20.

Imai, G., 1989. A unified theory of one dimensional consolidation with creep. Proceedings 12th International Conference Soil Mechanics Foundation Engineering 1, 57–60.

Jeeravipoolvarn, S., 2005. Compression behaviour of thixotropic oil sands tailings. Master's thesis, University of Alberta.

Kasperski, K. L., 1992. A review of properties and treatment of oil sands tailings. AOSTRA Journal of research 8, 11–52.

Kynch, G., 1952. A theory of sedimentation. Transactions of the Faraday Society 48, 166–176.

Liu, J., Lane, S., Cymbalisty, L., 1980. Filtration of hot water extraction process tailings. U.S. Patent 4225433, filed Oct 2,1978.

Masliyah, J. H., 2008. Oil sand extraction and upgrading-intensive short course. Department of Chemical and Materials Engineering, University of Alberta, Edmonton, AB, Canada.

McNabb, A., 1960. A mathematical treatment of one dimensional soil consolidation. Quarterly of Applied Mathematics 17, 337–347.

Nageswaran, S., 1983. Effect of gas bubbles on the seabed behaviour. Ph.D. thesis, Oxford University.

Olsen, H., Nichols, R., Rice, T., 1985. Low gradient permeability measurement in a triaxial system. Geoteqnique 35, 145–157.

Pollock, G. W., 1988. Large strain consolidation of oil sand tailings. Master's thesis, University of Alberta.

Raskin, L., Rittmann, B., Stahl, D. A., 1996. Competition and coexistence of sulfate-reducing and methanogenic populations in anaerobic biofilms. American Society for Microbiology, 3847–3857.

Richardson, J., Zaki, W., 1954. Sedimentation and fluidisation: Part 1. Instituition of Chemical Engineers 32, 35–53.

Schiffman, R., 2000. Theories of consolidation. University of Colorado at Boulder.

Schiffman, R., Pane, V., Sunara, V., 1985. Sedimentation and consolidation. Geotechnique 35, 69–72.

Schramm, L., Smith, R., 1989. Some parametric studies of oil sand conditioning in the hot water floatation process. AOSTRA 5, 87–107.

Sidique, T., Fedorak, P., MacKinnon, M. D., Foght, J. M., 2007. Metabolism of BTEX and naphtha compounds to methane in oil sands tailings. Environmental Science and Technology 41, 2350–2356.

Sills, G., Gonzalez, R., 2001. Consolidation of naturally gassy soft soil. Geotechnique 7, 629–639.

Sills, G., Wheeler, S., Thomas, S., Gardner, T., 1991. Behaviour of offshore soils containing gas bubbles. Geotechnique 41, 227–241.

Smith, R., Spence, J., Dai, Q., Chu, W., Wong, R., 1994. A laboratory comparison of the OSLO and Clark extraction process. part 2. Tech. rep., Syncrude.

Somogyi, F., Winnipeg 1980. Large strain consolidation of fine grained slurries. Presented at Canadian Society for Civil Engineers.

Steinour, H. H., 1944. Rate of sedimentation: Nonflocculated suspensions of uniform spheres. Industrial and Engineering Chemistry 36, 618–624.

Suthaker, N., 1995. Geotechnis of oil sand fine tailings. Ph.D. thesis, University of Alberta.

Tan, S., 1989. A simple automatic falling head permeameter. Soils and Foundations 29, 161–164.

Tang, J., 1997. Fundamental behaviour of composite tailings. Master's thesis, University of Alberta.

Terzaghi, K., 1924. Die theorie der hydrodynamischen spannungserscheinungen and ihr erdbautechnisches anwendungsgebiet. In: International Congress for Applied Mechanics.

Terzaghi, K., 1936. The shearing resistance of saturated clays. In: Proceeding of International Conference on Soil Mechanics and Foundation Engineering.

Terzaghi, K., 1943. Theoretical Soil Mechanics. John Wiley & Sons, Inc.

Thomas, S., 1987. The consolidation behaviour of gassy soil. Ph.D. thesis, Jesus College, Oxford.

Wheeler, S., 1986. The stress-strain behaviour of soils containing gas bubbles. Ph.D. thesis, Balliol College, Oxford.

Wichman, B., 1999. Consolidation behaviour of gassy mud: Theory and experimental validation. Ph.D. thesis, Delft University of Technology.

Yong, R., Siu, S., Sheeran, D., 1983. On the stability of suspended solids in settling ponds. part i, piece-wise linear consolidation analyst of sediment layer. Canadian Geotechnical Journal 20, 817–826.

Yong, R. N., Sethi, A. J., 1978. Mineral particle interaction control of tar sand sludge stability. Journal of Canadian Petroleum Technology 17, 76–83.

Znidarcic, D., Croce, P., Pane, V., Ko, H. Y., Olsen, Harold, W., Schiffrnan, R. L., 1984. The theory of one-dimensional consolidation of saturated clays: Part 3. existing testing procedures and analyses. Geotechnical testing journal 7, 123–133.